Optogalvanic effect in plasmas and gases

V. N. Ochkin, N. G. Preobrazhenskiĭ, N. N. Sobolev, and N. Ya. Shaparev

P. N. Lebedev Physics Institute, Academy of Sciences of the USSR, and Institute of Theoretical and Applied Mechanics, Siberian Branch of the Academy of Sciences of the USSR, Novosibirsk, and Computational Center of the Siberian Branch of the Academy of Sciences of the USSR, Krasnoyarsk
Usp. Fiz. Nauk **148**, 473–507 (March 1986)

The status of optogalvanic (OG) spectroscopy, involving a change in the impedance of a gas or plasma, with tunable lasers is examined. The main advantage of this approach over the usual absorption spectroscopy is its high sensitivity. The OG effect in plasmas, glow discharges, hf discharges, hollow cathodes, obstructed discharges, neutral gases, etc., is studied. Optogalvanic studies of the spectra of both the ground and excited states of atoms and vibrational-rotational and electronic transitions in molecules, nonlinear spectroscopic phenomena, and interference of degenerate states and the use of the optogalvanic effect for stabilization of laser frequencies are described. A great deal of attention is given to the physical mechanisms involved in the formation of the OG signal. The possibilities for employing the optogalvanic effect in quantitative spectroscopy are evaluated.

CONTENTS

1. INTRODUCTION

It is well known that absorption spectroscopy is a powerful tool for studying atomic and molecular structure and elementary processes, determining the concentrations of substances, diagnostics of different objects, etc. Quantitative measurements are based on the determination of the change in the intensity ΔI of light passing through the object. If the transmitted radiation has a high intensity, then its effect on the object must be taken into account, but ΔI remains the measured quantity.

An alternative approach is to record the change of some parameter of the object caused by the absorbed light. For gaseous and plasma objects the methods of laser-induced fluorescence and optoacoustical spectroscopy have been widely used, especially in recent years. The absorbed light gives rise either to excess fluorescence or a change in the density of the gas. The essential features of these methods, the basic areas of applications, and a bibliography are given, for example, in Ref. 1. Another approach, based on the light-induced change in the electric characteristics of the object, is mentioned in Ref. 1. In different articles this effect is called the optogalvanic (OG), optovoltaic, optoelectric, or ionization intensification effect. We shall adhere to the first name. The effect is caused by the fact that the absorption of light brings about a redistribution of the populations of the levels of atoms or molecules. As a result of different radiative and (or) collisional and (or) collective processes the density, mobility, and energy of the charged particles change, and this affects the ionization balance and conductivity of the object. Ionization occurs as a result of additional (with respect to absorption) processes. The dependence of the effect on the wavelength of the radiation has a resonant character. The conductivity can also vary simply because of photoprocesses, for example, photoionization (including multiphoton or stepped)[2,3] or nonresonant absorption.[4] In the final analysis the OGE is recorded based on the change in the current Δi or voltage ΔU in the electrical circuit including the object under study. The ratio γ of the magnitude of the change in the current or voltage in the external circuit to the

 0038-5670/86/030260-21$01.80

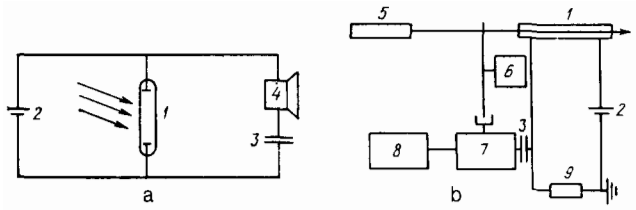

FIG. 1. Recording the OGE. a) Arrangement of Penning's experiment on the measurement of the frequency of sound from the loudspeaker with irradiation of the discharge. b) Block diagram of measurements employing a laser; 1) discharge; 2) High-voltage source; 3) capacitor; 4) loudspeaker; 5) laser; 6) modulator; 7) phase-sensitive detector; 8) recording device; 9) resistor.

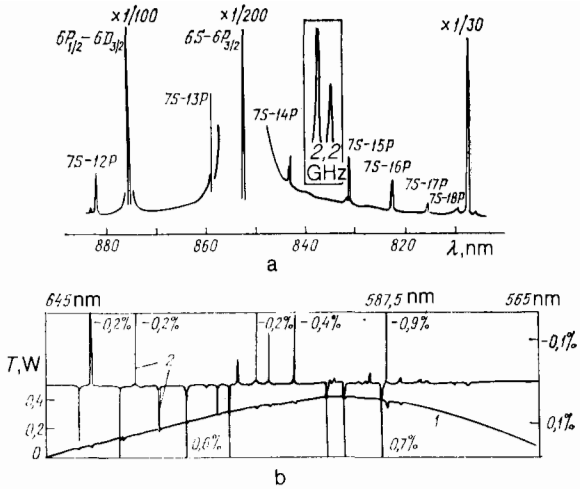

FIG. 2. Examples of OG spectra. a) OG spectrum of cesium[20]; voltage variation. b) *Spectra of a discharge in an He–Ne mixture.*[21] *Ordinate axes:* a) power of radiation passing through the discharge; b) relative changes in the voltage. 1) Optical spectrum, 2) OG spectrum. For lines of the spectrum 2 which do not fit into the field of the figure the magnitude of the OGE is indicated in percent.

energy of the absorbed light is also used as a measure of the OGE (optogalvanic effect). Such observations are most naturally performed in gas discharges, where they have been widely used.

The OGE was first observed by Foote and Mohler[5] in gases and by Penning[6] in a gas-discharge plasma. Penning observed that when a discharge in neon at a pressure of 20 Torr is irradiated by radiation from the same type of discharge the voltage from the discharge tube increases by an amount $\sim 10\%$. In order to demonstrate the OGE conveniently the discharge was connected into a circuit with a capacitor and a loudspeaker—the frequency of the sound changed when the discharge was illuminated (Fig. 1a). In later works the effect was discussed and studied primarily in order to determine the role of metastable states in stepped ionization processes.[7–9]

Stimulated by the requirements of absorption spectroscopy, the optogalvanic recording of signals in gases and plasma improved rapidly. It soon became clear that the OGE can be used not only as a convenient means for detecting absorption but also as a method for studying the characteristics of gaseous and plasma media.

Interest in OG phenomena has grown rapidly in recent years in connection with the development of laser technology. The OGE has been used to study processes in the active media of gas-discharge lasers and for stabilizing the lasing frequency. Another application was initiated in Refs. 10 and 11 and exploited in Refs. 12–14. It involves the use of frequency-tunable lasers for spectroscopic purposes. One of the main advantages of OG spectroscopy is its high sensitivity, which opens up prospects for studying the excited states of atoms, the detection of impurities, and other applications. An attractive feature of laser OG spectroscopy lies in the simplicity with which the signal is recorded: it is simply taken off the resistance in the power-supply circuit for the discharge into a phase-sensitive detector (Fig. 1b). A capacitor separates the constant high voltage. Continuous or pulsed lasers—dye,[12,15] color-center,[16,17] and diode[18]—are used, depending on the region of the spectrum and the experimental possibilities. Circuits with frequency multiplication are used.[19]

Figure 2a shows an example of the OG spectrum of Cs in a discharge with transillumination by a dye laser in the region 800–890 nm.[20] The high signal-to-noise ratio, even for very weak transitions, is interesting. Figure 2b shows the spectra in the region 565–645 nm, recorded by transilluminating a discharge in a mixture with an He–Ne laser.[21] The spectrum 1 is the usual absorption of laser power and the spectrum 2 was recorded using the OG recording scheme. It is evident that the OG method is very sensitive. It is also evident from Fig. 2b that the OG spectrum has a peculiarity distinguishing it from the usual optical spectrum. In the optical spectrum all lines correspond to the absorption of light, whereas in the OG spectrum the sign of ΔU is different for different lines. It is clear that the interpretation of such a spectrum requires a detailed analysis of the mechanism of its formation.

In recent years a large number of studies of both the nature of the OGE and its applications have been performed. Generalizing studies have also appeared for separate aspects of the problem (see, for example, Refs. 22 and 23). The purpose of this review is to describe the present status of research on laser-induced OG phenomena in gases and plasmas and their possible applications.

2. PHYSICAL MECHANISMS FOR THE FORMATION OF THE OPTOGALVANIC EFFECT (OGE)

The first investigations[6–8] were of a qualitative character only. In Ref. 6 the observed OGE was used to confirm the presence of the Penning mechanism of ionization

$$Ne^M + Ar \rightarrow Ne + Ar^+ + e, \qquad (1)$$

where Ne^M is the group of metastable states of neon lying above the ionization energy of Ar. When the discharge is irradiated atoms are excited from the state Ne^M into highly excited states, which can decay bypassing the state Ne^M and slow down the reaction (1). Other experiments showed, however, that the OGE also occurs in a discharge in pure neon, which is probably attributable to the illumination-in-

duced attenuation of the stepped ionization by electrons through Ne^M. In subsequent investigations[7,8] experiments were performed with spectral resolution, and they revealed that the magnitude of the OGE depends on the conditions in the discharge and on the type of optical transition. In all experiments[6–8] a positive effect $\Delta U > 0$ was observed.

Studies performed in recent years with the help of lasers revealed a number of new features of the phenomenon and have markedly expanded the range of objects studied. In describing the mechanism of the OGE, roughly speaking, two general stages can be distinguished. First, it is necessary to determine how the absorption of light brings about a change in the density and (or) the energy of charged particles. Second, a relationship must be established between these changes and the change in the macroscopic characteristics of the object and parameters of the electric circuit. The first part of the problem requires a kinetic approach; the second part requires a knowledge of the model of the object and the response of the circuit to perturbations of the charge density and charge mobility, though, of course, both parts are coupled to one another. We shall examine the OGE in different types of objects.

2.1. Glow discharge

Investigations of OGE in the positive column of glow discharges with different geometry have been described. Usually discharge tubes ~2–10 mm in diameter and a positive column ~100 mm long are used. The discharge current is equal to 1–100 mA, the gas pressure is equal to 0.1–5 Torr, and the ballast resistor, which also serves as the measuring resistor, is equal to 1–100 kΩ. The voltage on the dc current source is 100–1000 V. In order that the beam pass into the positive column the electrodes are placed in side arms, but coaxial structures are also used. The typical magnitude of the ac voltage obtained by transillumination with a modulated radiation of power $\sim 10^{-1}$ W is equal to $\sim 10^{-2}$ V. Longer discharges are also used (for example, 300 mm[16]). The OGE is also observed under transverse transillumination of the discharge (for example, Ref. 24).

The light-induced change in the characteristics of the positive column of the discharge can be described by the following system of equations:

The equation of balance for the electron density

$$\frac{dn_e}{dt} = G(n_e, N_j, T_e). \qquad (2)$$

The function G includes the creation and annihilation of charged particles and T_e is the electron temperature.

The equation of balance for the density of atomic states N_j

$$\frac{dN_j}{dt} = K_j(n_e, N_j, T_e, I_{nm}) \qquad (j, n, m = 1, \ldots, r). \qquad (3)$$

The function K_j describes the flow of atoms into and out of the level j, r is the number of discrete states taken into account, and I_{nm} is the intensity of the transilluminating radiation at the frequency of the transition $n \to m$.

The equation of energy balance for electrons is

$$\frac{d}{dt}\left(\frac{3}{2} kT_e\right) = \frac{\sigma(T_e, n_e)}{n_e} E^2 - \Phi_1 + \Phi_2, \qquad (4)$$

where the first term on the right describes Joule heating, Φ_1 represents the elastic and inelastic energy losses, Φ_2 describes the heating of electrons accompanying deexcitation of the excited atoms, σ is the conductivity of the plasma, k is Boltzmann's constant, and E is the intensity of the axial electric field.

The system is closed by the current equation

$$i = \sigma(T_e, n_e) E. \qquad (5)$$

The presence of resonance absorption of light from an external source, giving rise to the OGE and included in (3), augments in our case the usual models of the positive column.[25]

It should be noted that the apparent simplicity of the system (2)–(5) masks the complicated nonlinear dependences of G, K, σ, Φ_1, and Φ_2 on many parameters. In addition, the number of balance equations for (3) may in any specific situation be quite large. The mathematical complexities involved in solving the system are associated with the property of "rigidity," which imposes special requirements on the numerical algorithm.

The magnitude of the OGE with stationary resonance excitation of Na vapor in Ar buffer gas was first calculated in Ref. 26. It was assumed that $r = 2$, $\Phi_2 = 0$, and Φ_1 determines the ionization of the Na atoms, while n_e remains unchanged with $i = \text{const}$. It was assumed that the external radiation increases the role of stepped ionization, which decreases T_e, Φ_1, and, in accordance with (3), the intensity E. Numerical calculations showed that E can decrease by tens of percent for radiation intensities exceeding the saturation level and an Na density corresponding to a temperature of 650–800 K.

The fact that the OGE with $i = \text{const}$ changes n_e was taken into account later,[27] and the following expression was obtained for the change in the field:

$$\Delta E = 1.96 \frac{2m_e kT_e}{\pi e^2 R^2 \lambda_e n_e} i \left(\frac{\Delta T_e}{2T_e} - \frac{\Delta n_e}{n_e}\right); \qquad (6)$$

where m_e, e, and λ_e are the electron mass, charge, and mean-free path; ΔT_e and Δn_e are the illumination-induced changes in the electron temperature and density; and, R is the radius of the discharge tube. The values of n_e, T_e, Δn_e, and ΔT_e can be obtained by solving the system (2)–(5). Figure 3a shows the computed values of Δn_e, ΔT_e, and ΔE as a function of the intensity of the radiation transilluminating the discharge in Na vapor. The experimental data for ΔE, which are in good agreement with the calculations, are also presented.

We note that electron energy losses to ionization of impurity atoms play a determining role in the energy balance when the electron density is low. As the density is increased electron excitation of atoms becomes important.[25] This factor, as well as the superelastic heating of electrons (the term Φ_2 in (4)) was taken into account in Ref. 4. The calculations showed that when $P > 10^{-3}$ Torr electronic excitation constitutes the larger part of the energy losses, while superelastic heating can compete with Joule heating.

The change in the field intensity in the positive column brings about a change in the current which depends on the

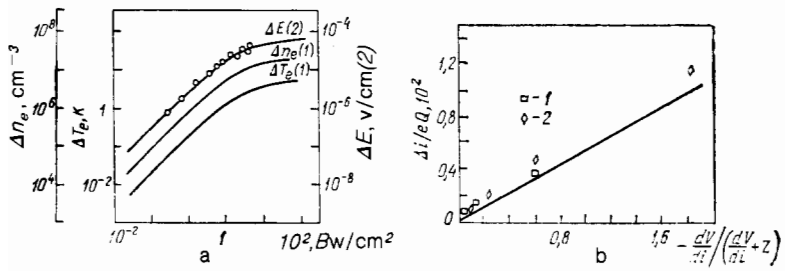

FIG. 3. Computed (solid lines) and experimental (symbols) data for the stationary OGE in a glow discharge. a) The change in the electron density Δn_e, the electron temperature ΔT_e, and the field intensity ΔE as a function of the intensity of radiation with $\lambda = 589$ nm[27]; discharge in an Ne–Na mixture. $P_{Ne} = 50$ Torr, $i = 5$ mA, $N_{Na} = 4.35 \cdot 10^9$ cm^{-3}, $T_e = 20400$ K, $E = 3.7$ V/cm. b) The change in the current Δi in a discharge in helium[28]; $\lambda = 587.6$ nm, $RP_{He} = 0.05$ cm·Torr; 1—$Z = 118$ kΩ, $i = 4, 6, 8, 12$, mA; 2—$Z = 208; 118, 58; 33$ kΩ; $i = 6$ mA.

form of the glow discharge. For a normal discharge the cathodic voltage drop V_c does not change when the current changes. For this reason, the increase (decrease) of the voltage drop in the positive column of length l is equal to the decrease (increase) of the voltage drop on the resistance Z of the external circuit:

$$\Delta i = -\frac{l\Delta E}{Z}. \qquad (7)$$

In an anomalous discharge a change in the voltage drop in the positive column gives rise to a change in the cathodic voltage drop. If the voltage on the discharge tube remains constant, then

$$\Delta i = -\alpha l \Delta E, \quad \alpha = \frac{\partial f(V_c)}{\partial V_c}, \qquad (8)$$

where $f(V_c)$ is the current-voltage characteristic of the discharge.

A simple linear model of the stationary OGE induced in a normal discharge in helium by radiation with wavelength $\lambda = 587.6$ nm (the transition 2^3P–3^3D) was constructed in Ref. 28. It is based on the equations of balance of charge (2) and current (5). The formation of charge in the absence of radiation is determined by the two-step electron ionization of atoms; charge annihilation is determined by free collisions with the wall. Under the action of the radiation (in the absence of saturation) the efficiency of ionization for one absorbed photon is determined by the ratio of the associative ionization rate a of He (3^3D) to its spontaneous decay rate A. As a result

$$\Delta i = -\frac{a}{A} Q \frac{eR\mu E}{0{,}77l\,(2kT_e/m_i)^{1/2}} \frac{dV/di}{(dV/di)+Z}; \qquad (9)$$

where Q is the number of photons absorbed per second, μ is the electron mobility, m_i is the ion mass, and dV/di is the dynamic resistance of the positive column. The parameters of a glow discharge in helium have been studied in great detail, and the absorbed radiation energy and the value of dV/di are easily measured. Figure 3b shows the computed and experimental data for Δi for several values of i and Z. The values of a, A, μ, and T_e were taken from the published data, E and dV/di were measured, $l = 13.5$ cm, and $R = 0.1$ cm. It is evident that the calculation is in satisfactory agreement with experiment. This model was later[29] used to describe the OGE on the $1s_5$–$2p_4$ ($\lambda = 594.5$ nm) transition in a discharge in neon. In this case the difference between the calculations and the experimental data is larger than in helium, reaching 100% and higher. This is probably attributable to the more complicated structure of the atomic terms and the lower reliability of the data on the probabilities of elementary processes and discharge parameters. Volume recombination of charged particles and the change in the electron temperature could play an appreciable role.

An anomalous discharge was studied in Refs. 4 and 30. It is believed that the relaxation time of the conductivity of the positive column is longer than the relaxation time of the cathodic region and the change in the current "follows" the state of the positive column. The solution of (2)–(5) in the Schottky approximation, taking into account (8), gives the expression[30]

$$\frac{dt}{dt} = \frac{\alpha l i E}{i + \alpha l E}\left[\sum_{j=1}^{r} n_j S_j - D_a\left(\frac{2{,}4}{R}\right)^2 - \frac{1}{T_e}\frac{dT_e}{dt}\right]; \qquad (10)$$

where S_j is the coefficient of electronic ionization of atoms from the state j and D_a is the coefficient of ambipolar diffusion. The first two terms on the right side of (10) describe the change in the electron density and the last term describes the change in the mobility of the electrons. The expression (10) is useful in that it enables evaluating the ratio of the contributions of different processes to the OGE. The results of the numerical solution of the system (2)–(5), (8) are on the whole in agreement with the experimental data for impulsive excitation of Ne and Na vapor.[4,30] Figure 4 shows the behavior of the current in the OGE for three transitions in neon $1s_i$–$2p_j$ excited by short laser pulses. Analysis based on (10) shows that the first peaks of the pulse for the cases of Figs. 4a and b are determined by the increase in the stepped

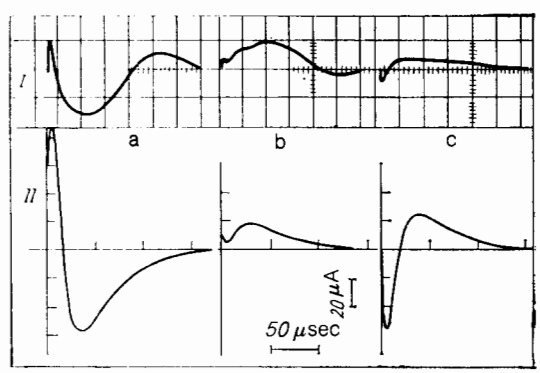

FIG. 4. The behavior of the current accompanying excitation of neon in a glow discharge.[30] I) experiment, II) calculation. The scales of all figures are the same. a—$\lambda = 633.4$ nm ($1s_5 - 2p_8$); b—$\lambda = 650.6$ nm ($1s_4 - 2p_8$); c—$\lambda = 659.9$ nm ($1s_2 - 2p_2$), $R = 0.4$ cm, $l = 1$ cm, $P_{Ne} = 1$ Torr, $i = 10$ mA, $\alpha = 6.7 \cdot 10^{-3}$ A/V^{-1}, the duration of the exciting pulse is equal to 10^{-8} s and the power is equal to $\sim 10^4$ W.

ionization from the $2p_8$ level. The initial negative response for the case of Fig. 4c is determined by the decrease in the electron mobility. The subsequent negative and positive responses are caused primarily by changes in the populations of the metastable states.

We can thus say that the proposed theoretical models of the OGE in the positive column of normal and anomalous glow discharges are on the whole satisfactorily described by the observed changes in the electrical parameters, at least for comparatively simple atomic systems. Of course, it is premature to use the indicated models as a basis for the solution of a wide complex of inverse diagnostic problems of OG spectroscopy. Although methods for diagnostics of nonequilibrium gas-discharge plasma based on OG spectra can in principle be developed (some examples will be presented below), further serious investigations are still required here.

Experiments with obstructed glow discharges are of interest. The length of the discharge is short, and the region of the cathodic drop forms the largest part.[31] Ionization is obstructed and the current is transported primarily by ions, which, however, are created by electrons. An insignificant change in the rate at which electrons are knocked out of the cathode therefore appreciably affects the current. The effect of the irradiation on the current can be manifested through the annihilation of metastable atoms, which are active in knocking electrons out of the surface. This situation was exploited by Doughty and Lawler.[32] They studied the OGE on the $\lambda = 594.5$ nm line of neon. The discharge gap was 1 cm long and the electrodes consisted of 3×10 cm^2 plates. Large plates are necessary in order to record the weak absorption of the radiation transilluminating the discharge in a direction normal to the propagation of the current. The magnitude of γ for the OGE (the ratio of the power of the OGE signal, liberated in the external circuit, to the absorbed light power) depends on the electrode material and is much higher than in the positive column. Among the metals studied (steel, stainless steel, Cu, brass, Mo, and Al) the largest effect is observed with Al and brass. For the $\lambda = 594.5$ nm line of neon in the positive column $\gamma = -3 - -6$,[32] in a hollow cathode $\gamma \sim -10$ (see Ref. 33), and in an obstructed discharge $\gamma \sim -400$. The minus sign corresponds to a reduction of the current accompanying irradiation.

A marked increase in the OGE when recording the spectra of molecular ions N_2^+ and CO^+ in the region of the cathodic dark space was also observed in Ref. 34. In this region the sensitivity of the OG method is much higher than that of the method of laser-induced fluorescence, but is lower than the latter method in the region of negative luminescence (an ion density of $\sim 5 \cdot 10^9$ cm^{-3}). Walkup *et al.* ascribe the high sensitivity of the OG detection of ions to the effect of excitation on the mobility of the ions, which occurs because the ion-neutral charge-exchange cross section of the excited ions is lower than that of unexcited ions.

2.2. Discharge in a hollow cathode

This type of discharge is widely used in studies of atomic OG spectra. Lamps with a hollow cathode are commercially available and have been developed for exciting the resonance transitions of most atoms, primarily for atomic-absorption spectroscopy and analysis. The theory of discharges with a hollow cathode has not been adequately developed, and the interpretation of the OGE in them is based, as a rule, on qualitative or semiempirical considerations. In particular, the question of which of the mechanisms—selective ionization or heating of electrons—makes the determining contribution to the OGE is being debated. The phenomenological approach to the decription of this situation on the basis of selective ionization is considered in Refs. 35–37. The "multiplication factor" β, determining the number of electrons emitted by the cathode as a result of a number of processes brought about by one precursor electron, is introduced. In the stationary case $\beta = 1$. The change in the discharge voltage accompanying radiation-induced excitation is expressed in terms of the starting difference in the populations of the levels, the relaxation times of these levels, and the derivatives of β with respect to the voltage and the population of the levels. These quantities are fixed based on the requirement that the best correspondence be obtained with the experimental data on the development of OGE in a time interval up to 10^{-4} sec. The number of relaxation times required is justified qualitatively. In so doing, it is often possible to describe in a very detailed fashion the development of the OGE. This approach has the deficiency that many (up to four in neon) relaxation times are not explicitly related to the specific physical processes, and the approximation of the experimental dependences is to a certain extent formal. The description of the sign-alternating OGE with the help of inverted states also requires justification. Thus, inversion is not required in order to interpret the curves in Fig. 4 for a glow discharge.

A description of the OGE in a hollow cathode based on the heating of electrons in type II collisions is given, for example, in Refs. 38–40. The estimates presented in Ref. 40 for the excitation of uranium show that the change in the conductivity is primarily attributable to heating of electrons, and $\Delta T_e / T_e \sim 3 \cdot 10^{-3}$. The same estimates show that selective ionization is 10 to 100 times weaker. The heating mechanism is supported by experiments[3] on the excitation of U II, giving rise to simultaneous amplification of the emission lines of U I. Mass-spectrometric experiments[41] with a hollow cathode with neon, which show a correlation between the changes in the voltage and the density of Ne^+ under the action of the radiation, provide evidence against the idea that heating of the electrons is exclusively responsible for the formation of the OGE. There are objections to[42] and support for[43] the idea that the efficiency of the OGE is independent of the ionization potential of the atom, which is an argument in favor of the heating mechanism. Summing up, it is evident that further studies must be performed in order to clarify the picture of the OGE in a hollow cathode.

2.3. Discharge with high-frequency excitation

The OGE can be observed by transilluminating an electrodeless discharge.[44–46] The signal is recorded either in the circuit supplying power to the discharge or with the help of a special antenna. The employment of hf discharges rather

than dc discharges for OG spectroscopy can be more advantageous because it is possible to work with gases and radicals that interact with the electrode metal, it is possible to obtain a more "pure" plasma, and low-pressure discharges are stable. Thus studies[15] of the predissociation of HCO showed that these radicals are observed by the OG method only in an hf discharge (in CH_3CO). We also note the important possibility of increasing the signal-to-noise ratio with frequency modulation of the discharge.[46,47] But, there is less experience in working with such discharges than with dc discharges.

Attempts to construct at least a simplified model of the OGE have recently been made in connection with the indicated advantages of hf discharges.[48,39] For this Eqs. (2)–(4) are supplemented by the quasistationary Maxwell equations taking into account the skin layer.[50] Discussion of the boundary conditions and the details of the solution of the system are presented in Ref. 49. We merely point out the fact that Eqs. (3) take into account collisional mixing and electronic ionization (recombination is neglected), diffusion and radiation transport of excitation (including also radiation trapping), and external illumination. In Eqs. (2) and (4), ambipolar diffusion, the electronic thermal conductivity, the total electronic ionization from all levels of the neutral component, the external hf field, and inelastic collisions are taken into account for the electronic component. The change in the specific energy input Q of the hf field into the plasma is used as a measure of the OGE. Here, in the approximation under study, if the volume of the plasma is V, then

$$Q = V^{-1}\int_V \sigma\,|\,\mathbf{E}\,|^2\,dV \sim n_e^{-1/2}, \qquad \frac{\Delta Q}{Q} \sim \frac{\Delta T_e}{T_e}. \qquad (11)$$

Model numerical calculations of the OGE in an hf discharge were carried out in Refs. 40 and 49 for an atom with two bound states. Figure 5 shows the radial profiles $n_e(r)$ and $T_e(r)$ for a plasma without illumination and with a saturating level of the external radiation power entirely filling the plasma. The increase in n_e corresponds to the drop in T_e; in addition, the maximum of T_e at the periphery of the tube is, for all practical purposes, not displaced. Figure 6 shows the integral characteristic of the OGE $\Delta Q/Q$ as a function of the

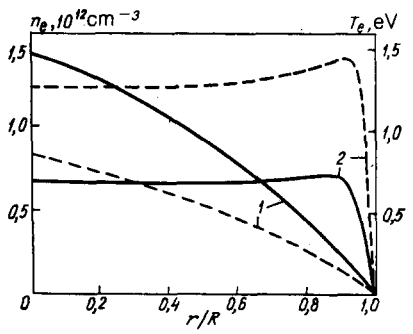

FIG. 5. Model calculations[49] of the radial distributions of n_e and T_e in hf discharges in a tube with radius R. The cross section for inelastic processes is equal to 10^{-15} cm^2, the ionization potential is equal to 10 eV, the excitation energy of the resonance level is equal to 5 eV, and $R = 1$ cm. The broken curves are for the case with no external illumination and the solid curves are for the case of saturating illumination. 1) n_e; 2) T_e.

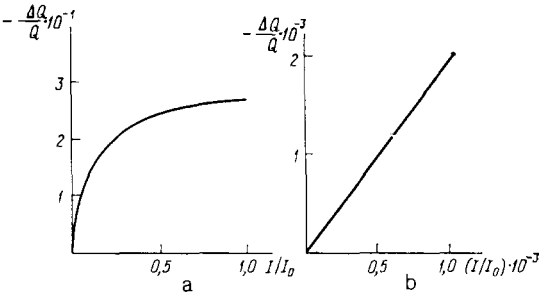

FIG. 6. Change in the specific energy input into the hf field in the presence of the OGE as a function of the intensity of the transilluminating radiation. I_0 is the saturation intensity. See Fig. 5 for the starting data. Figures a and b differ in their scales.

intensity of the transilluminating radiation. The initial part of the curve (Fig. 6b) is practically linear (this is confirmed analytically in Ref. 49). The latter is important for quantitative OG spectroscopy.

The described model,[48,49] based on numerical calculations, can be further developed and refined. At this stage it is important to obtain experimental results, of which there are still few, concerning the mechanism of the OGE in an hf discharge.

2.4. Flames

Beginning with Ref. 12 the OGE in flames is studied primarily in connection with the determination of the concentrations of elements and diagnostics of combustion processes.[51–55] Ionization in a flame occurs in the absence of an external field also. Electrodes are inserted into the flame and voltage is applied to them in order to detect the excess ionization produced by the transillumination. A configuration in which one of the electrodes serves as the burner housing is often used.

The OGE in a flame is usually attributed to the fact that transillumination at the frequency of the resonance transition repopulates the excited state, lowers the ionization energy, and increases the ionization rate constant following Arrhenius's law. This, in its turn, can substantially reduce the density of neutral atoms in the zone of the laser beam; this was observed experimentally for Na atoms.[55] The question of the mechanism by which the excess ionization is recorded is important in the interpretation of the OGE signal. The OGE under impulsive irradiation of the flame is modelled in Refs. 55 and 56. The formation of a nonstationary OGE signal in a flame is linked with the induction of charge on electrodes accompanying the spatial separation of the electrodes and ions in an external field. In Ref. 53 the nonmonotonic dependence of the OGE signal is explained qualitatively by means of an analysis of ambipolar diffusion in an external field.

In Ref. 57 the OGE in a flame is recorded by probing the flame with a microwave field. The attenuation η of the microwave field with frequency ω is given by

$$\eta \sim \frac{e^2 n}{mc}\,\frac{\nu}{\omega^2+\nu^2},$$

where n and m are the density and mass of the charges, and ν

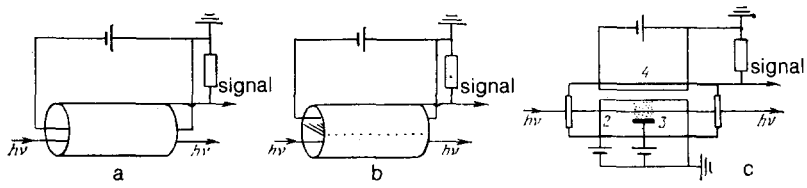

FIG. 7. Thermionic diodes. a) Ordinary diode. b) Ordinary diode with a screening grid; c) double diode; 1) tube, 2 and 3) cathode and anode of the exciting diode, 4) detecting diode.

is the frequency of collisions between charged particles and other particles. Electrons make the main contribution to absorption. Increasing $\omega > \nu$ decreases absorption, which imposes an upper limit on ω. The lower limit is associated with the spatial resolution, which is of the order of the wavelength of the field. Since it is technically comparatively simple to record relative changes of microwave power of 10^{-3} with a full power of ~ 1 mW, elementary estimates show that such probing does not introduce appreciable perturbations. This is one of the advantages of the method over the usual method, where the potential on the electrodes is usually $\sim 10^3$ V, which perturbs the charged component. Another advantage is associated with analytical applications and consists of a reduction of the limit of detectability of the elements. Preliminary experiments[57] with Na show that this gain constitutes $\sim 10^3$.

In interpreting OG measurements in flames the possibility of multiphoton ionization, for example in the detection of the radicals of PO and NO,[58] or stepped photoionization, as suggested in the interpretation of the OGE on the lines of alkali metals, must be taken into account.[53,59] The reaction of radiatively excited alkali-metal atoms with electronegative molecules[60] $M^* + XY \rightarrow M^+ + XY^-$ can also occur.

2.5. Thermionic diodes

This device (also known as a thermionic converter or diode with space charge) was used as a detector of ions and excited atoms in Refs. 61 and 62. In its simplest form it consists of a heated wire (the cathode) and an anode, separated from the cathode by several millimeters and usually consisting of a cylinder surrounding the cathode (Fig. 7a). The emission from the cathode creates a region with negative space charge. The electrons can overcome this potential barrier and a current will flow in the diode circuit without the imposition of a voltage, if the electrode materials have different work functions. If an ion enters the space-charge region, then, moving toward the cathode, it lowers the barrier, which is manifested as an increase in the current flowing through the diode. The diode forms a trap for the ion, which cannot escape through the ends of the diode, since the lower temperature at the ends of the wire lowers the space-charge density. The low electron-ion recombination cross sections ensure that the residence time of the ion in the volume will be long. As a result, the device has a high sensitivity, and experiments[63] show that the current changes already exceed the noise when 10 ions per second enter the diode.

A thermionic diode was first used for spectroscopy in Ref. 5. Some aspects of the spectroscopy of highly excited states using these devices are described in Ref. 64. In high-resolution spectroscopy, especially for highly excited Rydberg levels, the space-charge field can give rise to Stark excitation. To avoid this in Ref. 66 the diode is separated by a screening grid (Fig. 7b). The atoms are excited in the bottom region screened from the field and diffuse into the space-charge region. In working with alkaline-earth elements, however, when high temperatures are required in order to achieve the required particle density, emission appears in practically all elements of the structure. This causes the field of the charges to have an appreciable effect on levels with $n \gtrsim 100$. To proceed into the region with $n \gtrsim 100$ a ring-shaped diode in which not one but several heated wires arranged symmetrically relative to the axis are used was proposed in Ref. 66. Because of the symmetry the field virtually vanishes on the axis of the diode. A double thermionic diode was proposed in Ref. 67 (Fig. 7c). The idea consists of preexciting the atoms in the discharge and then studying the absorption spectra. The structure is enclosed in a heated steel tube 1. The exciting diode consists of a heated cathode 2 and an anode 3—a metallic plate, located at a distance of 3–4 mm from the cathode. The constant voltage (several volts with a metal-vapor pressure of $\sim 10^{-1}$ Torr in an inert buffer gas at a pressure of $\sim 10^{-1}$ Torr) creates a weak glow discharge, which is transilluminated by a laser beam. The atoms excited by the light are ionized either in the discharge or in the region of the space charge of the second thermionic diode, where they are detected. The employment of a double diode ensures a 10^2–10^3 times higher sensitivity than that obtained with the OGE in a glow discharge. Thus a comparison of the contours of the Sr lines of the transition $5s5p\,^1P_1$–$5s7s\,^1S_0$, obtained by detection with a thermionic diode and by direct recording of the OGE in the exciting diode under optimal conditions of the discharge, shows that the signal-to-noise ratio is increased by ~ 400.[67]

2.6. Molecular-gas plasma

Investigations of the OGE on molecular transitions are conducted both in the visible and in the IR regions of the spectrum. In the visible region of transitions between electronic states the measurement technique is analogous to that used in studies of atomic spectra. There is also a general analogy between the mechanisms of the OGE on electronic transitions in molecules and on atomic transitions.

Diode lasers with a wide continuous-tuning band and gas molecular lasers with discrete tuning on lines are used in the IR region. Figure 8 shows examples of OG spectra of molecules in the visible and IR regions.[22] Spectra can be recorded reliably even with diode IR laser powers of ~ 1 mW.

The vibrational energy of a molecule (~ 0.1–0.3 eV) is much lower than the ionization energy (several eV), and the

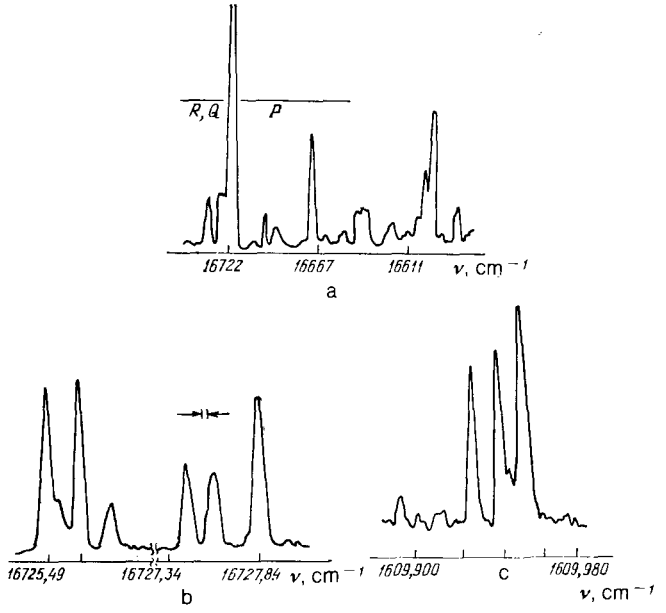

FIG. 8. Examples of OG spectra of molecules in a glow discharge.[22] a, b) Spectra of NH_2, discharge in NH_3 under a pressure of 1.8 Torr, dye laser. c) Spectrum of No_2, discharge in NO_2–He at a pressure of 1.2 Torr, diode laser.

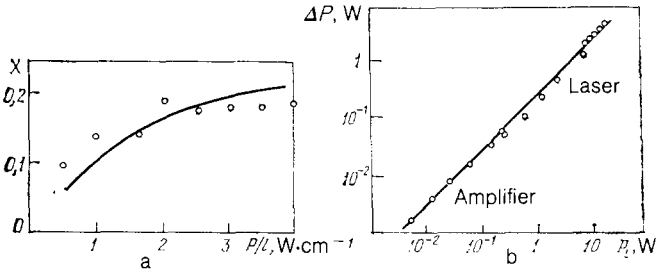

FIG. 9. Comparison of measurements with the predictions of a model of thermal perturbations for the active medium of a CO_2 laser and an amplifier.[69] The circles show the experimental points and the curves show the model calculations. a) The dependence of the "coefficient of the OGE" x on the power input per unit length of the discharge P/l. b) Change in the power input into the discharge ΔP as a function of the power P_l extracted from the discharge by the laser radiation.

mechanism of the OGE associated with the reduction of the ionization threshold by the excitation of atoms and molecules in the visible region of the spectrum is hardly effective here. Keeping this in mind, a mechanism associated with vibrational relaxation was proposed in Refs. 19 and 68. The energy in the vibrational-rotational states excited by the radiation is transformed into heat by means of collisions, and the gas density decreases. This reduces the electron energy lost in collisions between electrons and molecules, i.e., both acoustic and ionization mechanisms exist. The time constant of the effect is determined by the relaxation times of the vibrational levels. The frequency-phase characteristics of the OGE in the active medium of a CO_2 laser were studied in Ref. 68 as a function of the frequency of modulation of the lasing intensity. A correspondence was established between the modulation frequencies, characteristic for changes in the amplitude and phase of the OGE, and the relaxation times of the levels of the asymmetric and bending modes of CO_2, between which the laser transition occurs.

The stationary OGE in the active medium of the CO_2 laser was studied quantitatively in Ref. 69 based on the indicated model. It was assumed that the change in the electron losses, associated with the change in the gas density, occurs only as a result of the change in the collision frequency, but not as a result of the efficiency and ratio of the channels for collision losses. When the discharge current is maintained constant the relative change in the power $\Delta P/P$ injected into the discharge under the action of the radiation is given by

$$\frac{\Delta P}{P}=\frac{\Delta P_c}{P_c}=\frac{\Delta n_e}{n_e}=\frac{\Delta T}{T},$$

where $P_c = n_e \nu_c E_c$ are the electron energy losses in collisions with heavy particles per second; ν_c is the collision frequency; E_c is the average energy lost in a collision; and T is the temperature of the gas. The power carried away from the discharge by the laser radiation can be related to the change in the injected power:

$$\Delta P=\frac{1+R}{1-R} X\gamma_{\text{loss}} P_L, \qquad (12)$$

where R is the coefficient of reflection of the semitransparent mirror; γ_{loss} is the loss factor of the cavity; P_L is the lasing power; $X=\{2[(T_w/T_d)+1]\}^{-1}$ is the "coefficient of the OGE"; $T_d = T - T_w$, where T_w is the temperature of the wall in the discharge. The quantities T_d, P_L, and P are measured and T_w is known. The losses γ_{loss} are evaluated from the known values of R, the losses in the optics and apertures, and also the measured gain of the medium and the lasing threshold. Figure 9a shows the curves of X versus the power injected per unit length of the discharge. The solid curve corresponds to values of X with the measured values of T_d, and the circles show the values of X calculated from (12) with the measured values of ΔP, P_L, and γ_{loss}. Figure 9b shows the dependence of the change in the power ΔP on the change in the power P_l, extracted by the laser radiation from the discharge. The region $P_l \gtrsim 1$ W corresponds to measurements in a CO_2 laser, while the region $P_l \lesssim 1$ W corresponds to measurements in a CO_2 amplifier, the discharge conditions which are identical to those in the laser. The circles show the experimental values, and the solid line corresponds to the dependence $P_l = \Delta P[(T_w/P_d)+1]$, following from the model. Agreement is obtained with the power varying by four orders of magnitude. Thus in spite of its *a priori* nature and simplifications the model of thermal perturbations[18,68,69] describes the OGE in a complex object such as the active medium of a CO_2 laser, while the relation (12) can be useful for determining the parameters characterizing the operation of the CO_2 laser. It has been proposed[69] that the model is also applicable to other IR molecular lasers.

The existence of an acoustic mechanism in the formation of the OG signal on IR transitions in molecules is confirmed by experiments[19,70,71] in which the OGE accompanying transillumination of the gas on the resonance transitions outside the discharge zone was studied.

A different model of the OGE in a CO_2 laser, analogous

to models for discharges in atomic gases, was studied in Ref. 72. It is believed that generation affects the rate of stepped ionization through the state N_2 ($B^3\Pi$). This model, however, does not explain a number of experimental facts and there are objections to it.[73]

We note that in a complicated system such as a gas discharge the different parameters are interrelated. When one parameter changes, the others change also. Acoustic effects accompanying transillumination are also present in discharges in atomic gases.[74] In atomic gases, however, these effects are spinoffs in the first approximation, while in molecular gases they are a significant part of the mechanism of the OGE.

2.7. The OGE with a change in the discharge conditions

There are many observations of the effect of the discharge conditions on the magnitude of the OGE (ΔU). An important feature is that the polarity of the OGE changes when the conditions change, even for a fixed transition. Figure 10 shows the OGE as a function of the discharge current (hollow cathode) in Ne [75] for three wavelengths. For example, the sign of the OGE induced by radiation with $\lambda = 603.0$ nm changes twice. A qualitative explanation for the dependences are proposed in Ref. 75 based, in the general case, on a five-level scheme, which is explained in Fig. 11; here M is a metastable level (M), H is a highly excited level (H), R is a resonance level (R), G is the ground state (G), and the + sign marks the ionization limit. The solid straight arrows indicate ionization and deionization processes in the absence of irradiation. The wavy arrows mark the transition induced by the radiation. The dashed arrow tips indicate the direction of the radiation-induced changes in the rates of the processes. The double tips indicate a faster process.

a) The transition H–H. Ionization proceeds more rapidly from the higher state, $\Delta U < 0$.

b) The transition M–H, weak discharge current. The radiation excites the atom from the metastable state into the excited state. H can decay along different channels, including bypassing M. An increase in the population of H does not compensate the weakening of the ionization from M, $\Delta U > 0$.

c) The transition M–H, strong discharge current. The population of M is saturated when the current is increased, but the population of H continues to increase, so that the rate of ionization from H is higher than from M. The destruction of M and the population of H by radiation on the whole increase the rate of ionization, $\Delta U < 0$.

d) The transition R–H, the discharge current is weak. The electron density is low and does not allow for a coupling between R and M. The case is analogous to a), $\Delta U < 0$.

e) The transition R–H, the electronic density is high enough for mixing of R and M, but is still too low to produce an appreciable population of H. Just as in the case b), the weakening of the ionization owing to destruction of R (and together with it M also) is not compensated by an increase in the ionization from H, $\Delta U > 0$.

f) The transition R–H. The electronic density is high and ensures not only mixing of R and M, but also a high population of H. The situation is the same as in the case c), $\Delta U < 0$.

This scheme explains the dependences in Fig. 10. The group of levels of the Ne (1s) configuration consists of two metastable and two resonance levels, and the nearest pairs of the three lowest ones are separated by ~ 0.05 eV, which enables their mixing by electrons. The transition $\lambda = 576.4$ nm always leads to $\Delta U < 0$ (case a). The transition $\lambda = 588.2$ nm corresponds to the case b) with weak currents and the

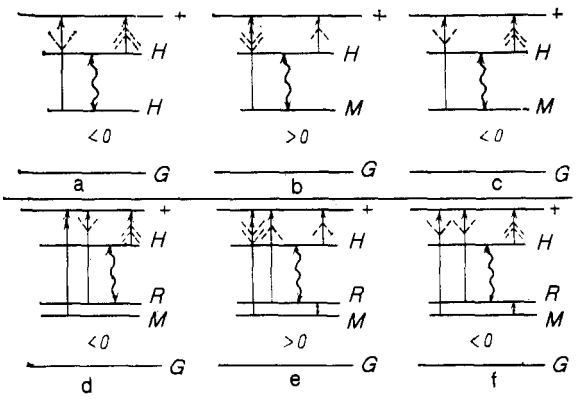

FIG. 11. Diagram clarifying the change in the sign of the OGE accompanying a change in the discharge current.[75]

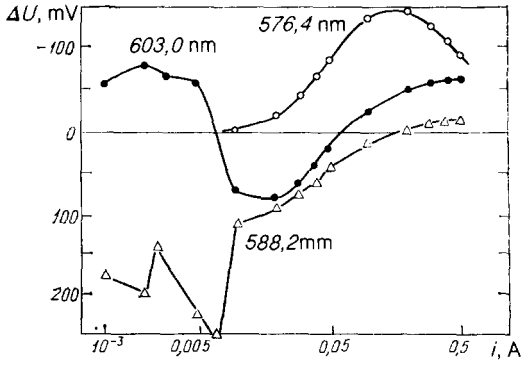

FIG. 10. The value of ΔU of the OGE as a function of the current in the hollow cathode for three wavelengths in Ne.[75]

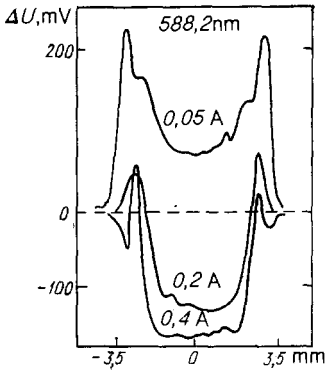

FIG. 12. Value of ΔU of the OGE as a function of the position of the transilluminating beam relative to the axis of the hollow cathode.[75] The neon pressure is equal to 5 Torr.

case c) with strong currents. The transition with $\lambda = 603.0$ nm gives rise to the OGE as the current is raised, corresponding to the cases d–f). The dependence of the OGE on the position of the transilluminating beam relative to the discharge axis is explained by the existence of a profile of the electron density. Examples of such dependences are shown in Fig. 12 for the Ne line $\lambda = 588.2$ nm.

2.8. The OGE in a rarefied gas

An interesting possibility for observing the OGE in a rarefied gas was recently discovered.[76] Let a quasimonochromatic wave propagate along the z axis and let it be absorbed in an inhomogeneously broadened transition. Only particles whose velocity projection $v_z \approx \Omega/k$, where Ω is the detuning from the central frequency of the contour of the line and k is the wave number, will interact with the radiation. When $\Omega \neq 0$, the excited particles acquire a directed velocity v_z. With subsequent ionization (for example, in an associative process) the velocity of the ions remains approximately constant. The modulus of the electron velocity can be much higher than Ω/k and the components v_x and v_y will also be large, as a result of which the electrons will escape to the walls. The ion current determines the OGE; in addition, unlike, for example, the mechanisms described in Refs. 77 and 68, the inhibiting volume collisions can be neglected. A simple estimate of the current accompanying absorption of radiation with a power of $\sim 10^{-2}$ W by the gas gives $i = 10^{-2}\,\xi$ (amperes), where ξ is the probability that the excited atom will be ionized. Modern instruments can record currents of $\lesssim 10^{-14}$ A, i.e., the OGE can be observed if $\xi \sim 10^{-12}$. In reality ξ is much higher. Thus for the reaction $2\mathrm{Na}\ (3p) \rightarrow \mathrm{Na}_2^+ + e$) the value of ξ, estimated from the known data (cross section of the process, lifetime of the resonance level, gas-light interaction volume, thermal velocity, etc.) is equal to $\sim 10^{-7}$, and $i \sim 10^{-9}$ A. An experiment[76] with Na vapor, in which measures were taken to suppress the direct photoeffect, demonstrated good agreement with theoretical estimates, and the OGE was reliably observed by means of the shift of the radiation frequency of the dye laser relative to the center of one of the D lines.

From the physical viewpoint this situation is interesting in that its study is free of the well-known difficulties associated with the construction of adequate models of the gas discharge. The limitations to such an approach, as compared with discharges, are associated with the fact that the OGE can be observed primarily with the absorption of particles in ground states.

3. OPTICAL SCHEMES FOR REALIZING THE OPTOGALVANIC (OG) EFFECT

The high monochromaticity, intensity, polarization, and directedness of laser beams enable realizing in OG spectroscopy practically all the advantages associated with these qualities, which also exist in the usual optical spectroscopy.

3.1. Counterpropagating-photon absorption resonances

When two counterpropagating photons, whose total energy is equal to the energy $\hbar\omega_0$ of an atomic transition, are

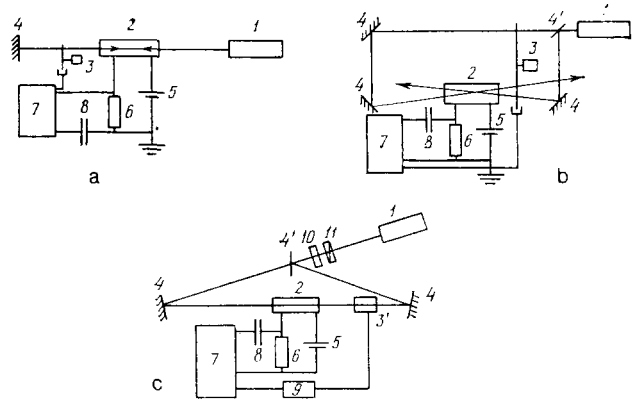

FIG. 13. Diagrams of experiments on the observation of narrow nonlinear resonances with the help of the OGE. a) Absorption of counterpropagating photons (TOGS). b) Saturated absorption (IMOGS). c) Polarization resonances (POLINEX). 1) Tunable laser; 2) discharge (or other object); 3) disk modulator; 3') polarization modulator; 4, 4') reflecting and semitransparent mirrors; 5) power supply; 6) resistance; 7) recording apparatus; 8) capacitor; 9) high-voltage amplifier; 10) quarter-wave plate; 11) polarizer.

simultaneously absorbed, narrow resonances appear in the Doppler-broadened line.[70] If the projection of the velocity of the atom on the propagation direction of the photons Z is equal to v_z, then the atom perceives the frequency ω of the counterpropagating waves as $\omega_1 = \omega + kv_z$ and $\omega_2 = \omega - kv_z$, respectively. The velocity of the atom does not appear in the resonance condition $\omega_0 = \omega_1 + \omega_2 = 2\omega$, i.e., Doppler broadening is compensated for the entire ensemble of atoms. The width of the resonance is determined by the homogeneous broadening of the transition.

The resonance is usually recorded from the fluorescence signal. In a plasma, however, such observations are prevented by the intrinsic fluorescence. In Ref. 80 it was proposed that the OGE in a glow discharge be used to detect resonances, while in Refs. 81 and 82 it was proposed that the OGE in a thermionic diode be used for this purpose. This method is often called TOGS (two-photon OG spectroscopy). A block diagram of the experiment is shown in Fig. 13a. Light from a tunable laser 1 passes through the discharge (this could also be a different object) and is reflected from the mirror 4, creating a standing wave in the discharge. The OG spectrum is recorded in the standard manner.

3.2. Saturated-absorption resonances

The formation of narrow nonlinear resonances in the Doppler-broadened contour is widely used in ultra-high-resolution spectroscopy.[79] The homogeneously broadened component is usually recorded from the absorption of the probing wave when its frequency in the system of coordinates fixed to the atom coincides with the pumping frequency. Measurements based on the resonant dip in the laser power as the frequency is scanned within the gain contour or on the resonant increase in power when the contour of the resonantly absorbing cell is scanned (inverted dip) are also possible.

The nonlinear resonance was first observed with the help of the OGE on the ($2p_4$–$4d_3$) transition in Ne.[21] A new

method of Doppler-free saturation spectroscopy based on the OGE (IMOGS—intermodulation OG spectroscopy) is proposed in Ref. 83. The arrangement of the experiment[83] is shown in Fig. 13b. The modulator disk contains openings corresponding to the frequencies f_1 and f_2 of modulation of the laser beams w and w'. Only particles which contribute (within the limits of homogeneous broadening) at the center of the Doppler contour can interact simultaneously with the two beams. This occurs with the modulation frequency $f_1 \pm f_2$, which is the reference frequency for the synchronous detector. The spectrum is recorded at this frequency. In contrast to TOGS, in IMOGS not the entire ensemble of atoms in the absorbing state participates in the formation of the OGE. Unlike the case of the OGE in a gas (see Sec. 2.8), however, the requirement that the velocity of a particle be conserved when the excited atom transforms into an ion is not imposed on the mechanism of ionization in a discharge. The directed motion of charges is formed by the external field.

Analysis[83] shows that the sensitivity of OG detection in saturated-absorption spectroscopy is approximately 10^2 times higher than that of measurements of the change in the intensity of the probing beam.

3.3. Polarization OG spectroscopy

In recent years the variants of OG spectroscopy employing in a substantial manner the polarization of the radiation interacting with the gas or the plasma have proved to be quite useful. In this case, the formation of the OG signals is based on effects such as optical orientation and alignment of atoms or molecules as well as level crossing when an external magnetic field is imposed on the discharge.

We shall first study the method of polarization intermodulation excitation—POLINEX,[84] which, aside from OG spectroscopy, can be combined both with fluorescence spectroscopy and optoacoustical detection. Unlike IMOGS, in this case the polarization characteristics of one or both beams from a frequency-tunable laser, as well as those of counterpropagating beams in a gas discharge, are modulated.

The typical arrangement of the experiment is shown in Fig. 13c. The polarization modulator can contain a Pockels cell or other devices; in addition, the modulation frequency (usually ~ 1 kHz) coincides with the frequency of the reference signal for the synchronous amplifier in the OG signal detection block. The beams interacting in the object can be circularly, linearly, or elliptically polarized.

The appearance of a narrow OG resonance in the POLINEX method can be understood from simple qualitative considerations. When a light quantum with the resonant frequency interacts with an individual atom in the case when the light is polarized the angular momentum of the photon is transferred to the atom, which changes the component of the magnetic moment of the atom to the direction of propagation of the light (orientation, alignment). In other words, the populations of the magnetic sublevels of the atom in the ground state are redistributed, and because of the well-known selection rules for absorption of a quantum this changes the transparency of the gas or plasma for the laser beam.[85,86]

By modulating the polarization of at least one of the counterpropagating beams we thereby periodically change the degree of orientation of the ensemble of atoms (molecules) and therefore the population of the excited state also, which generates an OG signal as a response to the difference in the absorption coefficients of the medium. Just as in the IMOGS method, this signal acquires a nonlinear subdoppler character (narrow peak) owing to the selection by the counterpropagating light beams of only those particles from the entire ensemble of atoms or molecules which have a virtually zero projection of the velocity on the direction of transillumination. POLINEX has the advantage that it efficiently exploits the process of collisional depolarization, which in most other high-resolution methods is a parasitic effect. The atoms, the projection of whose velocity on the quantization axis (the latter usually coincides with the direction of propagation of the beams) changes in collisions, no longer participate in the formation of the signal and do not contribute to the "pedestal" above which the useful signal rises. In addition, the method carries information not only about the particle concentrations, but also about the angular momenta of the levels between which the optical transition occurs, and also about the relaxation parameters of the light-induced orientation and alignment.[87–89]

In Refs. 84, 87, and 90 the possibilities of the POLINEX method were studied experimentally with the help of glow and hf discharges as well as a discharge with a hollow cathode. The OG detection of narrow nonlinear resonances obtained on the transitions He $2^3P - 3^3D$ ($\lambda = 587.5$ nm), Ne $1s_5 - 2p_2$ ($\lambda = 588.2$ nm), Ne $1s_5 - 2p_4$ ($\lambda = 594.5$ nm), Ne $1s_2 - 2p_1$ ($\lambda = 585.2$ nm), Cu $3d^{10}4p^2P_{1/2} - 3d^94s^2D_{3/2}$ ($\lambda = 578.2$ nm), has confirmed the great advantages of this method. The employment of hf discharges,[90] which in the POLINEX method ensure high signal-to-noise ratios under conditions of virtually complete elimination of the pedestal, is especially promising. The advantages of polarization modulation over the amplitude modulation are evident in Fig. 14. Similar results were obtained somewhat later in Ref. 91, where, in particular, the possibilities of the method for the little-studied problem of the hyperfine structure in atoms with an unfilled d shell (for example, molybdenum) are pointed out. A quite universal arrangement, enabling the realization of different variants of nonlinear subdoppler spectroscopy with both fluorescence and optogalvanic signal detection, is described in Ref. 91.

We shall now briefly discuss the possibilities of OG spectroscopy with level crossing. In recent years several methods for OG detection of crossing effects have been discovered. First of all, as shown in Refs. 88 and 92, the rate of impact ionization of excited atoms depends on the degree of alignment. In Ref. 93 this dependence was checked experimentally by placing gas-discharge neon tubes and thermoionic diodes in an external magnetic field of the order of 0.1 T. Although in Ref. 93 the theoretical models developed in Refs. 89 and 92 were checked indirectly (the phase shift of

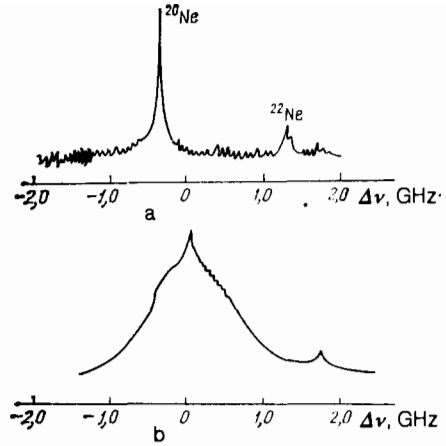

FIG. 14. The results of OG recording of sub-Doppler neon spectra (the $1s_5$–$2p_2$ transition, $\lambda = 588.2$ nm) in an hf discharge.[87] a) POLINEX method. b) IMOGS method.

the π and σ components for different values of the magnetic field was recorded), there are grounds for regarding the predicted effects as having been confirmed.

Second, the manifestations of the degeneracy of the states directly in terms of their populations can also be investigated entirely satisfactorily by the OG method. Here the intensity of the radiation must be close to saturation. The corresponding theoretical aspects are examined in Refs. 94 and 95. We shall not consider here the quite trivial case when the magnitude of the Zeeman splitting $\Delta\nu_H$ of the sublevels is comparable to the Doppler half-width and the detuning of the resonance brings about a natural drop in the absorption of the laser beam. A more interesting situation occurs when the external magnetic field is comparatively weak, so that $\Delta\nu_H$ is of the order of the inverse relaxation time of the coherence $2\Gamma_{AB}$, and then, systematically decreasing, gives rise to the case of a purely degenerate system (Fig. 15). We shall study on the basis of a convenient model[96] the transition between the A and B levels with total angular momenta $J_A = 0$ and $J_B = 1$; in addition, we shall assume that the radiation is linearly polarized normally to the direction of the magnetic field H, splitting the upper level into three magnetic sublevels $m_B = 0$ and ± 1. We neglect the collisional relaxation between sublevels. We shall compare three cases: a) $\Delta\nu_H > \Gamma_{AB}$, the radiation interacts with two groups of atoms with different velocities, and under conditions of saturation the population for J_B is equal to $n/2 + n/2 = n$; b) $\Gamma_{AB} > \Delta\nu_H > \Gamma_B$ (Γ_B is the homogeneous width of the upper level), the radiation interacts with one group of n atoms, the populations of the sublevels $m_A = 0$ and $m_B = +1$, $m_B = -1$ are equalized, so that the total saturated population of J_B is equal to $n/3 + n/3 = 2n/3$; and, c) $\Delta\nu_H = 0$, a coherent superposition of states occurs, so that σ^+ and σ^- transitions are perceived as one π transition, while the population of J_B is evidently equal to $n/2$. Thus when the magnetic field is scanned the change in the population of the upper level should be described by the convolution of Lorentzian profiles with widths Γ_{AB} and Γ_B. In typical cases Γ_{AB} constitutes approximately 1% of the Doppler width; Γ_B is an order of magnitude narrower. In the described simplified model the relative magnitude of these resonances is evidently the same: $S_1 = [n - (2n/3)]/n = 0.33$ and $S_2 = [(2n/3) - (n/2)]/(2n/3) = 0.25$.

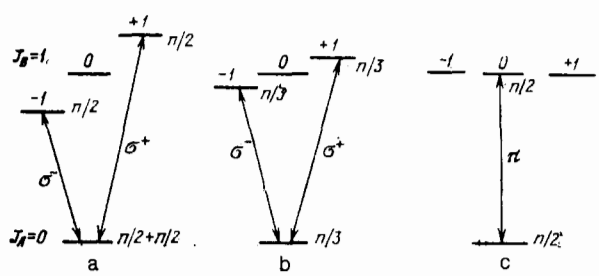

FIG. 15. Different cases of removal and restoration of the degeneracy of levels with $J_B = 1$. a—$T_{AB} < \Delta\nu_H$. b—$\Gamma_B < \Delta\nu_H < \Gamma_{AB}$. c—$\Delta\nu_H = 0$.

In a more detailed analysis the possibility of collisional mixing of the sublevels m_B, the incomplete saturation on the wings of the profile, trapping of radiation, the effect of optical pumping on the sublevels which do not directly interact with the radiation, etc., must be taken into account. All these questions await analysis; we only point out that the methods for taking into account trapping in the linear Hanle effect are discussed in Ref. 97.

As shown in Refs. 94–96, the basic consequences of the theoretical description of the form of the OG signal under the conditions of magnetic scanning are confirmed experimentally. In Ref. 96 a series of investigations of level crossing of atoms both in the absence of and in the presence of fields, carried out by the methods of OG spectroscopy, are described. The object of the investigation was a low-pressure discharge in Ne or Ar with an additional electrode for atomization (of Zr and Y). The method has the advantages that low values of the hyperfine interaction constants (magnitude and sign) can be determined and the atomic characteristics can be measured on very weak transitions, which cannot be done by the traditional methods of optical detection. In addition, in OG methods the requirements imposed on the frequency stabilization of the laser and the scanning technique are somewhat relaxed.

Interesting data on the mechanism for the increase in the lasing power of Ar^+ and Kr^+ continuous lasers accompanying the imposition of an axial magnetic field, discussed repeatedly in the literature, are presented in Ref. 95. A nontraditional explanation of the growth in the power in separate lines, associated not with the change in the electron density (usual interpretation), but rather with the nonlinear Hanle effect, is given.

3.4. Multiphoton and stepped excitation

At high radiation power multiphoton excitation can contribute to the OGE. This can be most important for particles with a high ionization potential. This mechanism has been observed, for example, in a flame.[98] The probability of the process depends, in particular, on the closeness of the real and intermediate virtual levels. Thus the detection of the two-photon effect accompanying absorption on the $He(2^3S)$

TABLE I. Increase in sensitivity with two-stepped excitation

Element	Cu	Fe	Na	Element	Cu	Fe	Na
E_i, cm^{-1}	62 317	63 700	41 449	λ_2, nm	453,1	538,3	568,8
E_0, cm^{-1}	11 203	7 377	0	E_2, cm^{-1}	52 849	53 353	34 549
λ_1, nm	510,6	364,8	589,0	Q_2, μJ	110	17	56
E_1, cm^{-1}	30 784	34 782	16 973	S_{1+2}, nA/ppb	0,016	0,07	1 000
Q_1, μJ	150	180	26	D, ppb	500	100	0,04
S_1, nA/ppb	10^{-5}	$4\cdot10^{-3}$	1,5	$\frac{S_{1+2}}{S_1}$	1 600	18	690
D, ppb	10^6	$2\cdot10^3$	6				

levels requires much higher power levels than for absorption in the levels of the 3s configuration of Ne. In helium the energy interval between the real and virtual levels is 10^2 times larger than in neon, which lowers the probability of the process by a factor of approximately 10^4.

Multiphoton ionization (MPI) is possible in strong light fields. MPI, detected by the change in the conductivity of the plasma, was observed, for example, in the detection of O and H atoms[20,99] and in the detection of PO and NO.[58]

The employment of two lasers for stepped excitation through the real levels requires much lower powers.[54,100,101] The simultaneous transillumination on two resonance transitions with a common level can substantially intensify the OGE as compared with the cases of transillumination at one of these frequencies separately (double resonance).

Table I compares the sensitivities and limits of detection of a number of elements in an air-hydrogen flame with one- and two-step schemes.[100] The sensitivity is measured in units of the current change per particle in an environment of 10^9 particles of the solvent (nA/ppb), and the limit of detection D is measured in particles per 10^9 particles of the solvent. Lasers at wavelengths λ_1 and λ_2 operate in the pulsed mode with energies of Q_1 and Q_2 per pulse. E_i is the ionization energy, E_0 is the energy of the starting state for excitation of the state E_1 by radiation with wavelength λ_1, and E_2 is the energy of the state excited from the state E_1 by radiation with wavelength λ_2. The increase in sensitivity with two-step excitation is ~ 10–10^3. In Refs. 102 and 103 attention is devoted primarily to the frequency selectivity of the double OG resonance, which is important for investigations of complex spectra. Different variants of the method, including one in which the upper or lower level is the common level, are studied in the same works. The case when two optical transitions have states with close energies, coupled by collisional exchange, is studied. This modification could be useful for studying relaxation processes. In Ref. 104 the OGE resonance with simultaneous transillumination of a plasma by a laser and microwave radiation (optical-microwave resonance) is studied.

3.5. Conditions for transillumination and localization of OGE

When the OGE is observed in a nonuniform object there arises the problem of finding the contribution of different zones. The solution in the two-dimensional case, when in different sections (x, y) normal to a chosen direction Z, the most important characteristics are conserved, is obvious. The object can be probed directly by transporting the beam parallel to Z. Such scanning was carried out, for example, in Refs. 4, 34, and 75 (see Fig. 12).

In the general three-dimensional case focusing of the laser beam gives definite results, this method was used, for example, in Ref. 105. The spatial resolution in this case is, however, low and it is difficult to guarantee that the unfocused part of the beam will not make a contribution.

Much better results are achieved with two-photon excitation in crossed laser beams. Thus in determining the concentration of H atoms in a flame[106] the L_α line was excited by two beams of light with wavelengths $\lambda_1 = 224$ nm and $\lambda_2 = 266$ nm. One of the beams (λ_1 or λ_2) is also responsible for the completion of the ionization process from the excited level. There also appears the possibility of monitoring the excitation and ionization processes independently, since the rate of one of the processes depends on the product and that of the other depends on the sum of the beam intensities.

The methods of subdoppler spectroscopy with intersection of beams (of course, usually at a small angle) can give comparatively good localization of the OGE.[47] The same is apparently also valid for OG detection of the degeneracy of levels, in particular, sections of the plasma can be separated by displacement in an external nonuniform magnetic field.

We note, finally, the possibility of transforming from the integral (with respect to the transillumination beams) OGE to a local OGE using a Radon transformation based on modern methods of computational tomography.[107,108] The principles of atomic-spectral tomography[109] employing a finite (for technical reasons) number of beams with the missing information obtained by frequency sweeping can also be used.

4. SOME APPLICATIONS OF THE OPTOGALVANIC EFFECT

4.1. Atomic OG spectroscopy

The optogalvanic spectra of a large number of elements, indicated below, have been studied. As the basis for this dis-

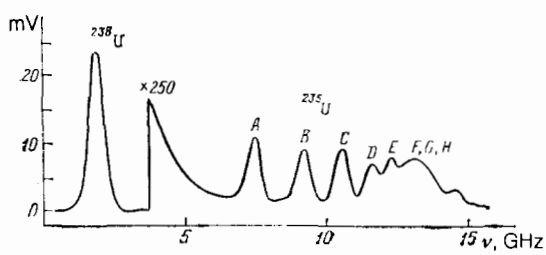

FIG. 16. The OG spectrum of uranium.[119] The letters mark the components of the hyperfine structure of ^{235}U.

cussion we took the data from Ref. 47 which we supplemented:

H (1, 5)						He (1, 3)
Li (3, 5)	Be (4)	B (5)		O (5)		Ne (1, 3)
Na (3—6)	Mg (4, 5)	Al (5)				Ar (1, 3)
K (3—5)	Ca (3—5)	Sc (5)	Ti (5), V (5)	Cr (5)	Mn (3, 5), Fe (5), Co (3—5), Ni (5)	
Cu (3, 5)		Ga (3—5)				Kr (1, 2)
Rb (4, 5)	Sr (1—3)	Y (3, 5)	Zr (3)	Mo (3)		
Ag (5)	Cd (5)	In (3)	Sn (5)			Xe (2)
Cs (1, 2, 4, 5)	Ba (1, 3—5)	La (3)				
Au (5)	Hg (1)	Tl (5)	Pb (5)	Bi (5)		
Sm (3)	Eu (3, 4)	Tu (5)	Yb (3, 4)	U (3)	Lu (5)	

The numbers in parentheses indicate objects in which the OGE was studied: 1) dc discharge tube, 2) hf discharge, 3) hollow cathode, 4) thermionic diode, 5) flame, 6) rarefied gas.

In addition to applied aspects (diagnostics, analysis, etc.), the OGE is also used to study atomic structures. The high sensitivity of the method determines the direction of these studies—spectroscopy of excited states, trace impurities, ions, transitions with low probabilities, etc., when the usual absorption and emission measurements cannot be performed because of the low signal-to-noise ratio. We shall confine our attention to individual examples.

The spectrum of the states of Ba in the region 5.2–7 eV is studied in Ref. 101. The energies for 636 new levels with principal quantum numbers up to $n = 45$ with $J = 0$–5 were identified and determined; in addition, the fine structure was resolved for levels with $n \leqslant 25$. The spectra of the Rydberg states of alkali metals have been studied. The energies of levels and isotopic shifts of ^{39,40,41}K (Refs. 110–113), ^{6,7}Li (Ref. 114), ^{85}Rb (Refs. 113 and 115), and ^{133}Cs (Ref. 116) have been determined. It was found that the dependence of the magnitude of the quantum defect on n for the nD_J series of cesium was found to be substantially nonmonotonic.[116] The isotopic shift in strontium ^{38,86}Sr has been studied for neutral and ionized atoms.[117]

It has been suggested that the high signal-to-noise ratio characteristic for the OGE even for very weak transitions be used in the future in experiments on the detection of parity nonconservation in the transition Cs(6s–7s).[20]

The OG spectrum of uranium in a hollow cathode was studied in Refs. 118 and 119. In spite of the low ^{235}U content ($\sim$0.3%) its spectra are reliably recorded. The OGE is also observed on the U II transitions. Figure 16 shows the spectrum of uranium in the region of 591.5 nm, where the components of the hyperfine structure (HFS) and the isotopic shift ^{235}U–^{238}U are resolved.

As the principal quantum number increases there appear effects caused by the perturbation of the levels accompanying the interaction of states converging to different ionization limits. Measurements for a large sequence of levels enable comparing data with existing theories. Thus it is noted in Ref. 120 that the experimental data for Ba do not correspond to the results of the multichannel theory of the quantum defect. The perturbation of the states strongly affects the nature of the HFS. The measurements are carried out primarily with Doppler-free resolution, and the HFS constants and the mixing of the states are determined (the first studies of the HFS of the transition ^{3}He(2^3p–3^3D) by the OG method were carried out by Lawler *et al.*[83]). For high levels, interactions of multiplet components with different principal quantum numbers but the same total angular momentum (n mixing) appear as the levels converge. The effect is observable when $n \gtrsim 100$ and has been recorded experimentally in the OG spectrum of Sr[66] (levels with $n \lesssim 160$ are recorded). In Refs. 121 and 122 the diamagnetic behavior of Rydberg states in external fields, when the Lorentz force acting on an external electron becomes comparable to the Coulomb interaction between the electron and the atomic core, was studied.

Some applications of the OGE in polarization spectroscopy have already been mentioned above.

4.2. Molecular OG spectroscopy

Though most publications concern studies of atomic spectra, there has now appeared a significant number of works on the study of molecular OG spectra. The main directions of these investigations have been recently reviewed in Refs. 22 and 123. Table II summarizes and supplements the results of Refs. 22 and 123. Just as in atomic spectroscopy, the advantages of OG recording of the spectra of molecules are manifested in transitions with low optical density. We shall confine our attention to several examples.

The investigations[15] of the structure of the absorption bands of the radicals of HCO in transitions terminating in the predissociation state are characteristic. The line widths give information on the probability of predissociation. Here the method of optical absorption cannot be used because of the low density of the radicals. It is estimated in Ref. 15 that the sensitivity of the OG method is approximately 10^5 times higher than that of the optical absorption method. Because HCO has a predissociative first excited state the method of laser fluorescence cannot be used. Optoacoustical detection

TABLE II. Investigation of molecular OG spectra

Molecules	Spectral region, nm	References	Remarks
Cs_2	620–650	11	Diode. First observations of molecular OG spectra.
In_2, Yb_2, CsKr, CsAr, Cs_2Kr	390–660	124–128	Diode. Electronic transitions of excimers and exciplexes. Hybrid resonances of the excitation of atoms through intermediate dissociative states of molecules.
LaO, YO, ScO	360–630	129	Flame. Identification of new transitions.
N_2	563–615	130	dc discharge. 1^+ system and Ledbetter bands $c_4'\Pi - a''^1\Sigma$
	598	45	Doppler-free resolution, hf discharge
	585–605	45, 131	hf discharge. Identification of new bands
	595–615	103	Hollow cathode. Double optical resonance. Identification of new bands.
H_2	573–610	130	dc discharge. Identification of new transitions between $2p^3\Pi$ states and states near the dissociation limit
I_2	520–630	132, 133	Weak-current dc discharge. B–X bands. Spatial resolution. Doppler-limited spectral resolution
	575–610	134	Medium resolution spectra
	532	133, 135	Diode. Determination of the energy of electron affinity
CO	640–660	136	$D^3\Delta - A^3\Pi$ bands
	550	137	Vibrational-rotational lasing transitions in the active medium of a CO laser
NH_2	570–615	130	dc discharge. First observations of free radicals
	596–605	22	Doppler-limited resolution, dc discharge
	580–610	131	hf discharge
NO_2	570–600	71, 130, 131	dc discharge. hf discharge
	6200	19	Diode IR laser. dc discharge
HCO	580–620	15	hf discharge in CH_3CO. Study of predissociation rates
CN	643–682	22	A–X bands
NH_3	9500	104	dc discharge, hollow cathode, hf discharge. N_2O laser: Doppler-free resolution. Double optical-microwave resonance.
	9500	19	Diode IR laser. dc discharge
	580–630	131	hf discharge
	11250–9200	70	hf discharge, CO_2 laser with discrete tuning
He_2	585–588	22	Rydberg transitions
CO_2	9300–10800	68, 138–140	Vibrational-rotational transitions in the active medium of a CO_2 laser
D_2O, H_2CO, SO_2, H_2S, H_2O_2	9700–9100	70	hf discharge. CO_2 laser with discrete tuning. Identification of transitions, searches for transitions for optically pumped far-IR lasers.
N_2^+	390	34	(0, 0) bands of the transition $X^2\Sigma - B^2\Sigma$. First observations of the OG spectra of molecular ions.
CO^+	490	34	(0, 0) band of the transition $X^2\Sigma - A^2\Pi$
NO	270–317	58	Flame. Multiphoton ionization.
PO	302–334	58	same

also cannot be used because of the low density and discharge noise.

The OG method was used to make the first identification of bands of the systems $b^1\Sigma_u^+ - a''^1\Sigma_g^+$ [103] and $c_5'^1\Sigma_u^+ - a''^1\Sigma_g^+$ [45] in N_2 and to obtain Doppler-free spectra of the Ledbetter bands $c_4'\Pi_u - a''^1\Sigma_g^+$.

Examples of OG spectra in the IR region, obtained with the help of diode lasers, are shown in Fig. 8. In Ref. 104 an N_2O laser, tunable in the above-threshold gain zone of the separated vibrational-rotational transition, was used to record the spectra of NH_3. The high lasing power (~ 1.5 W) enables obtaining comparatively simply the Doppler-free line shape of NH_3 under conditions of saturated absorption. The method of the double optical-microwave resonance, when the microwave frequency corresponds to the transition between the states of inversion doubling, is used in Ref. 104. The resonance-produced change in the magnitude of the OGE observed by sweeping the microwave frequency is, however, small because of the efficient collisional exchange between the levels, even at low gas densities.

4.3. Radiation detection

The employment of a discharge cell as a detector of resonance radiation was apparently first proposed and experimentally confirmed for the example of the IR line of helium $\lambda = 2058.1$ nm.[141] In Ref. 141 it was also proposed that the lines of Hg be detected by means of the OGE. Later experiments[142] showed that the selectivity of this method of detection is high (~ 0.1 cm^{-1}). If, for example, a hollow cathode filled with He^4 is used as the detector, then the radiation from an He^3-filled lamp is practically not observed. Using the high signal-to-noise ratio characteristic for the OGE and the high selectivity, Zalewski *et al.*[52] and Matveev *et al.*[143] used a gas-discharge cell to record the absorption of radiation in the method of intraresonance laser spectroscopy. The experiments showed that the limit of detection of such a detector is an order of magnitude lower than that of a photomultiplier.

4.4. Frequency stabilization of lasers and wavelength calibration

In active stabilization the lasing frequency of a laser is locked to some reference. A signal is fed from the photodetector into the feedback system (AFC). In continuous gas lasers this is usually carried out on the center of the gain line of the laser transition itself. An error signal for the AFC system is generated by modulation of the cavity length. The OGE enables the elimination of photodetectors, the active medium also plays the role of the detector. Such a scheme was first implemented in Ref. 138 in order to stabilize the lasing frequency of a gas-discharge CO_2 laser based on the center of the gain line. The characteristic changes in the voltage on the discharge tube, associated with the search signal, constituted ~ 10 V under the conditions of Ref. 138 or $\sim 0.25\%$ of the total voltage. An improved electronic scheme for stabilizing the lasing frequency of a CO_2 laser with the help of the OGE is described in Ref. 139. Optimization of the conditions enabled[68] realizing a long-term frequency instability of $\sim 5 \cdot 10^{-9}$. In Refs. 68, 138, and 139 lasers with low-pressure active media (10–30 Torr) were studied, whereas in Ref. 140 the frequency of a wave-guide CO_2 laser with a pressure of 180 Torr in the active medium was stabilized. In this case the sensitivity of the OGE is sufficient for ensuring a frequency instability of ~ 1 MHz (the relative instability is $\sim 10^{-8}$). Judging from the results obtained by different authors, the use of the OGE yields, in order of magnitude, the same values of the instabilities as those obtained using photodetectors. Investigations of the stabilization of the frequency of an He–Ne laser with the help of the OGE is discussed, for example, in Refs. 144 and 145.

The OGE is used for frequency stabilization of gas lasers not only in laboratory but now also in commercial lasers,[146] including in the domestically produced LG-74 CO_2 laser. In this stabilization scheme the gain contour of the lasing transition itself plays the role of the frequency discriminator. The discriminator in lasers with an inhomogeneously broadened transition can be enhanced by employing the Lamb dip or the inverted dip in a resonance absorption cell in the cavity.[79] A discharge cell outside the cavity can also be used.[147] Such cells are also used for stabilizing and measuring the lasing frequency of wide-band dye lasers.[148–150] The search signal is generated while sweeping the tilt angle of the intracavity etalon, while the error signal is generated in the usual manner on the synchronous detector. The characteristic signals at the input to the synchronous detector have magnitudes of 5–100 mV with lasing powers of 0.1–0.2 W. The stabilization in this case occurs on discrete frequencies from the tuning band. In Ref. 148 the lines of neon (588.2 nm), sodium (589 nm and 616.1 nm), and barium (553.5 nm) were used. The wavelength instability in this case did not exceed 10^{-5} nm (the relative frequency instability was $\sim 2 \cdot 10^{-8}$). Because of the multiplicity of resonance absorption lines in hollow cathodes this approach is very promising in the wavelength range of interest for dye lasers. It is noted in Ref. 20 that stabilization can be achieved even on lines with very weak absorption.

The question of spectral calibration and determination of the line width of tunable lasers was discussed in Ref. 151. For OG stabilization and measurement of the laser wavelength it is convenient to use a discharge with a hollow cathode with uranium lines[152] in the IR, visible, and UV regions. An automated system for performing calibration based on 25 lines in the region 580–800 nm with the help of a neon tube is discussed in Ref. 153.

The desirability of performing calibration based on the OG spectra of radicals in a discharge, in particular, for monitoring the composition of the atmosphere, is pointed out in Ref. 154. One of the possible paths for developing the method of OG stabilization and calibration of laser frequencies consists of employing intracavity discharge cells in a magnetic field. This enables controllable displacement of the frequency reference and generation of an error signal of the AFC system without parasitic modulation of the radiation while scanning the positions of the elements of the laser cavity.

4.5. Investigation of elementary processes

The discovery itself of the OGE in a discharge, as mentioned above, was linked with the investigation of Penning ionization processes[6] and processes of the type $A^* + A \rightarrow A_2^+ + e$, $A^* + A \rightarrow A_2^+ \rightarrow A^+ + A^-$. These processes are still being studied (see, for example, Ref. 155).

Processes occurring in electronegative gases are studied in Refs. 133, 135, and 156–158 by a method which is close to OG spectroscopy. The recorded electrical signal is generated by CO_2 laser radiation or by resonance Raman scattering of the light of a solid-state laser and a dye laser, and is explained by the fact that the rate of dissociative electron trapping depends on the degree of vibrational excitation of the molecule. The molecules SF_6, CCl_2F_2, I_2 were studied. The formation of negative ions accompanying collisions of optically excited Na (4d) atoms with O_2, SF_6, CH_3Br, CCl_2F_2 molecules were studied in Refs. 60 and 158 and the rate constants were determined. Analysis of the data led[60] to the conclusion that the Landau-Zener theory of nonadiabatic transitions in a system of molecular terms is applicable.

The OG method turns out to be effective for studying two-photon dissociation.[124–128] First, the molecule is excited into the repulsive or predissociative state; then the atom is photoexcited into a Rydberg state, from which it is ionized in thermal collisions. Even if the molecule has a wide excitation band, the resulting OGE is of a resonant character (hybrid resonances). This enables, in particular, the study of selective population of atomic states accompanying dissociation.

In Ref. 159 the OGE is used to study absorption in laser-induced collisions with dipole-dipole interaction, giving rise to redistribution of the particles over the levels:

$$\mathrm{Ba}\,(6s^2\,{}^1S_0) + \mathrm{Ba}\,(6s^2\,{}^1S_0) + h\nu\,(339{,}4\ \mathrm{nm}) \rightarrow \mathrm{Ba}\,(6p\,{}^1P_1) + \mathrm{Ba}\,(5d\,{}^1D_2),$$

$$\mathrm{Ba}\,(6s^2\,{}^1S_0) + \mathrm{He}\,(2s\,{}^1S_0) + h\nu\,(615{,}1\ \mathrm{nm}) \rightarrow \mathrm{He}\,(2p\,{}^1P_0) + \mathrm{Ba}\,(5d\,{}^1D_2),$$

and in addition this was the first observation of the last reaction. It has been proposed that this method also be used for

studying multipole interactions, multiphoton processes, and interactions with charge transfer accompanying collisions in a light field.

Doppler-free OG spectroscopy enables studying collisional line broadening and shifts (see, for example, Ref. 160). The probabilities of collisional excitation from Rydberg states of atoms have been measured.[161] We also mention investigations of reactions of particles with oriented spin moments,[162] the determination of the rates of vibrational relaxation of molecules[163] and energy of affinity in photodetachment of electrons,[164] etc., performed with the help of the OGE.

4.6. Quantitative plasma spectroscopy and plasma diagnostics

Available data indicate that, generally speaking, optical absorption and OG spectra are not similar to one another (see, for example, Fig. 2b and Ref. 165). This is attributable to the fact that the OGE depends not only on the quantity of light absorbed but also on the mechanism responsible for the change in the conductivity of the object with the participation of the upper level of the transition. From these qualitative considerations it may be expected that the similarity of optical and OG line spectra should be observed for transitions with a common upper level or when the upper levels are under very similar conditions. The last condition is met, for example, by molecular spectra with rotational fine structure. The system of rotational levels in a wide range of rotational quantum numbers, as a rule, is compact and efficiently "mixed" by collisions, which in ordinary spectroscopy is used for determining the gas temperature. These possibilities have not yet been investigated systematically. We call attention to the measurements[34] of the intensities in the rotational structure of OG spectra N_2^+ ($B^2\Sigma$, $v' = 0 \rightarrow X^2\Sigma$, $v = 0$) in an obstructed discharge. A 2:1 alternation of the intensities of the rotational lines in accordance with the nuclear spins was observed. The intensities of the sets of lines for ions with the same orientation of nuclear spins correspond to a Boltzmann distribution over the rotational levels. The magnitudes of the OG signals are proportional to the intensities of the transilluminating radiation. This definitely indicates the possibilities of quantitative investigations of a nonequilibrium plasma based on the OG line spectra.

The study of line profiles is an independent area of quantitative plasma spectroscopy and plasma diagnostics. Such investigations were already performed in the first publications on laser-assisted OG spectroscopy.[17,21] It was pointed out in Sec. 2.3 that the proportionality of the optical and OG line contours follows from the simple two-level model with low absorption in an hf discharge. For a two-level atom the condition of proportionality can also be obtained from Eqs. (2)–(5). This is confirmed experimentally in a number of articles and is used, in particular, for measuring the gas temperature based on the Doppler broadening (see, for example, Refs. 75 and 166). Studies in which the OG Doppler profiles of the lines of molecular ions with nonisotropic velocity distributions are determined are interesting. This work can apparently be extended so as to determine

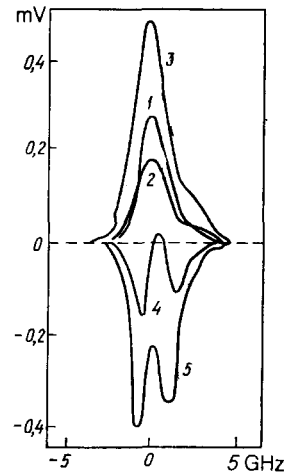

FIG. 17. The OG contours of the neon line for the transition $1s_2$–$2p_1$ at $\lambda = 585.2$ nm in a hollow cathode.[165] The pressure is equal to 3 Torr and the current (mA) is equal to 20 (1), 100 (2), 300 (3), 400 (4), and 450 (5).

the velocity fields of particles in different objects by means of the solution of the inverse problem, where the starting Doppler contour is, generally speaking, non-Gaussian, as is done in emission spectroscopy.[167] Together with this there exist data[165] indicating significant distortions of the OG contours. Figure 17 shows the profiles of the $\lambda = 585.2$ nm line of neon for different currents in the hollow cathode. For currents less than 100 mA the contours recorded by both the absorption method and the OG method coincide (the asymmetry at low currents is associated with the isotopic shift). As the current is increased the form of the OG contour changes markedly. The polarity changes and structure appears. Analogous effects were also observed in Ref. 19 for the IR region. It is pointed out in Ref. 165 that distortions are observed when the absorption of light by the plasma is comparatively high ($> 20\%$). At high optical densities the radiation at frequencies lying in the wings of the lines interacts efficiently with the plasma over the entire path of the beam, and the radiation at the frequency of the center of the transition gives rise to the OGE, appearing largely in the inlet zone of the beam. In a nonuniform plasma the resulting contour cannot be obtained by simple averaging over zones. At low optical densities the correspondence between the results based on absorption and on the OGE is satisfactory. Figure 18 shows the contours of the spectral lines of neon.[165] In the case of Fig. 18a the absorption in the transition $1s_5$–

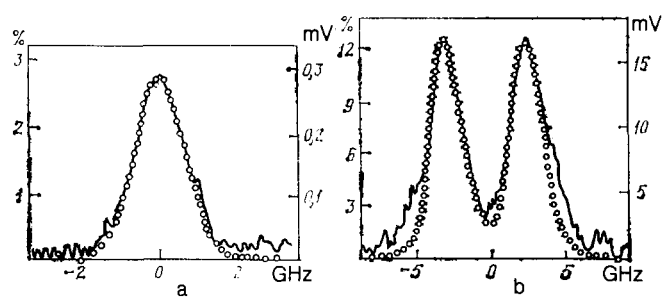

FIG. 18. Contours of neon lines. The solid curves show the optical absorption and the circles show the OG signal. a) Hollow cathode; the transition is $1s_5$–$2p_5$, $\lambda = 597.5$ nm; the current is equal to 50 mA; and the pressure is equal to 3 Torr. b) Indicator neon lamp; σ component of the transition $1s_5$–$2p_4$, $\lambda = 594.4$ nm; and the magnetic field is equal to 1600 G.

$2p_5$ is less than 3%. The discharge current in the hollow cathode is equal to 50 mA, and the pressure is equal to 3 Torr. The case of Fig. 18b corresponds to absorption in the Zeemann σ components of the transition $1s_5$–$2p_4$ in the indicator tube. The magnetic field is equal to 1600 G, the current is equal to 10 mA, and the absorption at the center is equal to 12%. The coincidence of the absorption and OG contours is satisfactory. The differences present are apparently associated with the low signal-to-noise ratio in the absorption measurements.

Thus experience shows that in many cases the OGE can be successfully employed for quantitative measurements and diagnostics of plasma. Applications involving the recording of line contours at low optical densities have the best validation at this stage.

4.7. Analysis of the composition of materials

The employment of the OGE for analytical purposes was first suggested in Ref. 168. Considering the high sensitivity of this method, this proposal is entirely natural.

The correspondence of the possibilities of the OG method and absorption spectroscopy or other, including laser (laser-induced fluorescence, laser acoustooptical detection) optical methods, Raman scattering or EPR methods, selective with respect to the energy states of atoms or molecules, can hardly be universal. It depends on the mechanism of the OGE, the type of transition and object in which it appears, and the schemes used to realize the OGE. For this reason, at this stage it is desirable to focus on the results achieved in practice.

Studies of hollow cathodes with Na, U, Eu, and Zr show[43] that the fluctuations of the current in the circuit supplying power to the hollow cathode with a finished construction correspond to random noise. This establishes the OG detection power $\sim 10^6$ cm^{-3} (or $\sim 10^2$ cm^{-3} in metastable states) for the indicated elements, which is in fact achieved in practice. In Ref. 169 the OGE was observed in a discharge in a hollow cathode and the absorption spectra of Ba^+ and Eu^+ ions were recorded.

Most analytical work by the OG method is done with the help of flames. This is attributable to the speed of the measurements, their simplicity, and the reproducibility of the results. The well-developed methods for injecting the material into the flame enable reliable calibration and virtually eliminate the difficulties associated with quantitative measurements in nonequilibrium objects, discussed in the preceding section. Table III shows the limits of detection for a number of elements by the OG method and the limits achieved by other methods. The data are taken primarily from Refs. 172–175. The following notation was employed for the methods: OG—optogalvanic, A—absorption, EM—

TABLE III. Limits of detection in flames[172–175]

Element	Wavelength of the OGE, nm	Limits of detection, ng/ml				
		OG	AB	EM	Fl_n	Fl_l
Ag	328,1	1	1	2	0,1	4
Al	309,3	0,1				
Au	242,8	1				
Ba	307,2	0,2	20	1	5	8
Bi	306,8	2	50	20 000	20	3
Ca	300,7	0,1	1	0,1	5	0,08
Cd	228,8	0,1				
Co	252,1	0,08				
Cr	298,6	2	2	2	0,5	1
Cr	301,8	2				
Cs	455,5	0,004				
Cu	282,4	100	1	0,1	8	1
Cu	324,8	100				
Fe	298,4	4				
Fe	302,1	2	4	5	10	30
Ga	287,4	0,07	50	10	100	0,9
Ga	294,4	0,1				
In	303,9	0,006	30	0,4		0,2
K	404,4	0,1				
Li	610,4	0,012				
Li	639,3	0,4				
Li	670,8	0,001	1	0,02		0,5
Lu	308,2	0,2	1	0,02		0,5
Mg	285,2	0,1	0,1	5	0,1	0,2
Mn	279,5	0,02	0,8	1	1	0,4
Na	285,3	0,05	0,8	0,1		0,1
Na	589,0	0,01				
Ni	300,2	0,08	5	20	3	2
Pb	280,2	0,6	10	100	10	13
Pb	283,3	0,09				
Rb	420,2	0,1				
Sc	301,9	0,2				
Sn	284,0	0,3				
Sn	286,3	2	20	100	50	
Sr	460,7	0,4				
Tl	291,8	0,09	20	20	8	
Ti	295,6	600				4
Tu	297,3	200				

emission, FL_n—fluorescence employing noncoherent light sources, and FL_l—fluorescence employing lasers. The typical limits of detection fall in the range 10^{-3}–10^2 ng/ml. In many cases, for example, for Pb, transitions between excited states give lower limits of detection than transitions from the ground state. In many cases the limits of detection by the OG method are appreciably lower than those achieved in other methods, and concentration linearity is obtained in the range 10^4–10^5 and higher. It is estimated in Ref. 173 that the limit of detection associated with electrical noise in the flame is equal to $\sim 10^5$ cm^{-3}. This limit has been achieved for Li.

This method of analysis is being developed in the direction of optimization of the excitation and recording schemes and the geometry of the object. The effect of the configuration of the electrodes and the flow velocity and composition of the gas are under study and methods of recording are being compared: based on the total voltage drop, the probe potential, and microwave absorption. An analytical device[174] for working with elements in the region 217–700 nm and having a dynamic range of not less than 10^4 has been developed.

5. CONCLUSIONS

The optogalvanic effect in plasmas and gases, which already has a long history, has been resurrected after the early work on the employment of lasers for its observation. The rapid growth of the interest in and the number of publications on this subject has already made, in a short period of time, the OG method a fundamental method for studying plasma media. The OGE is also employed to influence actively the properties of objects, as, for example, for the stabilization of laser frequencies and power or for cooling of plasma[30] and for isotope separation (see, for example, Refs. 13, 176, and 177), which were not discussed in this review. The OGE is now a subject of discussion at special conferences. With respect to the breadth of its aspects and applications the OGE in plasmas and gases is probably comparable to the photoelectric spectroscopy of impurities in semiconductors[178] and other well-known applications of the photoconductivity of solids.[179] In this review, however, it was impossible to compare in detail these physically related situations.

An important advantage of the OG method of recording is its high sensitivity to and selectivity of the quantum states of particles. For this reason, the practice of investigations and applications of the OGE, including those for studies of elementary processes, diagnostics, structures of atoms and molecules, etc., will undoubtedly expand. In many cases the OG method can be used in combination with traditional methods. The potential possibilities of OG methods are far from being exhausted. The question of the sensitivity of the OG method and the limiting signal-to-noise ratios, as compared with the methods of direct absorption measurements, laser-induced fluorescence, optoacoustical measurements, etc., nevertheless deserves further detailed and careful analysis. General considerations in this direction were put forth in Ref. 22, where, in addition, the advantages of the OG method were underscored. However, the limitations of the method, associated with the noise, have not been adequately studied and have been studied only for some particular cases of discharges in a hollow cathode[43] and some states of the positive column of a glow discharge.[180,181]

It is appropriate to underscore the fact that the methods of OG spectroscopy described in this review join closely in many cases with other methods, which differ somewhat with regard to their experimental implementation and have been under intensive development in recent years. Among these methods we mention first of all the methods of multistep photoionization spectroscopy, which have unique possibilities and which enable detecting single atoms and molecules.[182–184] The aforementioned methods[60,133,135,157,158] with direct detection of ions should apparently be included here also.

The quite simple nature of the effect is combined with the complex and many-branched mechanism responsible for the formation of the OG signal, especially under nonequilibrium conditions. A quantitative description can, for the time being, be given only for some very simple cases and objects. Further experimental studies must be performed and theoretical models of the phenomena observed must be constructed, which will undoubtedly lead to new possibilities and the further development of already-mentioned ones.

The authors thank V. S. Vorob'ev, E. A. Yukov, and Yu. Ya. Kuzyakov for useful discussions as well as Yu. B. Udalov and S. N. Tskhaĭ for assistance in selecting the references.

[1]N. Omenetto [Ed.], Analytic Laser Spectroscopy, Wiley, N. Y., 1979 [Russ. Transl., Mir, M., 1982].
[2]B. H. Rockney, T. A. Cool, and E. R. Grant, Chem. Phys. Lett. **87**, 141 (1982).
[3]W. G. Mallard, J. H. Miller, and K. C. Smyth, J. Chem. Phys. **76**, 3483 (1982).
[4]N. K. Zaĭtsev and N. Ya. Shaparev, Preprints No. 207-209F, Institute of Physics of the Siberian Branch of the USSR Academy of Sciences, Krasnoyarsk (1982).
[5]P. D. Foote and F. L. Mohler, Phys. Rev. **26**, 195 (1925).
[6]F. M. Penning, Physica **8**, 137 (1928).
[7]C. Kenty, Phys. Rev. **80**, 95 (1950).
[8]K. W. Meissner and W. F. Miller, *Ibid.* **92**, 896 (1953).
[9]Yu. Z. Ionikh, N. P. Penkin, and A. V. Samson, Vestn. LGU, Ser. fiz., khim., No. 4, (1), 51 (1976).
[10]C. B. Collins, B. W. Johnson, D. Popescu, G. Musa, M. L. Pascu, and I. Popescu, Phys. Rev. A **8**, 2197 (1973).
[11]D. Popescu, M. L. Pascu, C. B. Collins, B. W. Johnson, and I. Popescu, *Ibid.*, p. 1666.
[12]R. B. Green, R. A. Keller, G. G. Luther, P. K. Shenk, and J. C. Travis, Appl. Phys. Lett. **29**, 727 (1976); J. Amer. Chem. Soc. **68**, 1517 (1976).
[13]W. B. Bridjes, J. Opt. Soc. Am. **68**, 352 (1978).
[14]N. K. Zaĭtsev and N. Ya. Shaparev, Inventor's Certificate No. 678948 (USSR, 1977); Byull. Izobr., No. 29, 283 (1981).
[15]R. Vasudev and R. N. Zare, J. Chem. Phys. **76**, 5267 (1982).
[16]S. A. M. Al-Chalabi, R. S. Stewart, R. Illingvorth, and I. S. Ruddock, J. Phys. D **16**, 115 (1983).
[17]D. J. Jackson, E. Arimondo, J. E. Lawler, and T. W. Hansh, Opt. Commun. **33**, 51 (1980).
[18]R. C. Webster and R. T. Mensies, J. Chem. Phys. **78**, 2121 (1983).
[19]J. E. M. Goldsmyth, *Ibid.*, p. 1610.
[20]L. Ph. Roesh, Opt. Commun. **44**, 259 (1983).
[21]T. F. Johnston, Laser Focus **14**, 58 (1978).
[22]R. C. Webster and C. T. Rettner, *Ibid.* **19**, 41 (1983).
[23]J. E. M. Goldsmyth and J. E. Lawler, Contemp. Phys. **22**, 235 (1981).
[24]R. C. Webster, Rev. Sci. Instr. **54**, 1454 (1983).
[25]V. L. Granovskiĭ, Élektricheskiĭ tok v gaze (Flow of Electric Current in Gases), Nauka, Moscow (1971).
[26]D. M. Pepper, IEEE J. Quantum Electron. **QE-11**, 971 (1978).
[27]M. Maeda, Y. Moniyama, and Y. Miyazoe, Opt. Commun. **39**, 64 (1981).

[28]J. E. Lawler, Phys. Rev. A **22**, 1025 (1980).
[29]D. K. Doughty and J. E. Lawler, *Ibid.* A **28**, 773 (1983).
[30]N. Ya. Shaparev, N. K. Zaĭtsev, and V. A. Pushkarev, Preprint No. 274F, L. V. Kirenskiĭ Institute of Physics, Siberian Branch of the USSR Academy of Sciences, Krasnoyarsk, 1984.
[31]A. H. von Engel, Ionized Gases, Clarendon Press, Oxford, 1955 [Russ. Transl., Inostr. Lit., M., 1959, p. 244].
[32]D. K. Doughty and J. E. Lawler, Appl. Phys. Lett. **42**, 234 (1983).
[33]E. F. Zalewski, R. A. Keller, and R. Engelman, J. Chem. Phys. **70**, 1015 (1979).
[34]R. Walkup, R. W. Dreufus, and Ph. Avouris, Phys. Rev. Lett. **50**, 1846 (1983).
[35]G. Erez, S. Lavi, and E. Miron, IEEE J. Quantum Electron. **QE-15**, 1328 (1979).
[36]R. Shuker, A. Ben-Amar, and G. Erez, Opt. Commun. **42**, 1982 (1982); J. de Phys. **44**, C7-35 (1983).
[37]A. Ben-Amar, G. Frez, and R. Shuker, J. Appl. Phys. **54**, 3688 (1983).
[38]C. Dreze, Y. Demers, and J. M. Gagne, J. Opt. Soc. Am. **72**, 912 (1982).
[39]J. M. Gagne, Y. Demers, P. Pianarosa, and C. Dreze, J. Phys. (Paris) **44**, C7-355 (1983).
[40]R. A. Keller, B. E. Warner, E. F. Zalewski, P. Dyer, R. Engleman Jr., and B. A. Palmer, *Ibid.*, C7-23.
[41]K. C. Smyth, R. A. Keller, and E. F. Crim, Chem. Phys. Lett. **55**, 473 (1978).
[42]N. S. Kopeika, Appl. Opt. **21**, 3989 (1982).
[43]R. A. Keller and E. F. Zalewski, *Ibid.* **19**, 3301 (1980).
[44]C. Stanciulescu, R. Bobulescu, A. Surmeian, D. Popescu, I. Popescu, and C. B. Collins, Appl. Phys. Lett. **37**, 888 (1980).
[45]T. Suzuki and M. Kakimoto, J. Mol. Spectr. **93**, 423 (1982).
[46]T. Suzuki, Opt. Commun. **38**, 364 (1981).
[47]P. Camus, J. Phys. (Paris) **44**, C7-87 (1983).
[48]A. E. Bulyshev and N. G. Preobrazhensky in: XII SPIG-84: Contributed Papers, Sibenik, Yugoslavia (1984), p. 481.
[49]A. E. Bulyshev and N. G. Preobrazhenskiĭ, Dokl. Akad. Nauk SSSR **279**, 1357 (1984) [Sov. Phys. Dokl. **29**, 1034 (1984)].
[50]B. B. Henriksen, D. R. Keefer, and M. H. Clarkson, J. Appl. Phys. **42**, 5460 (1971).
[51]M. A. Nippolt and R. B. Green, Appl. Opt. **20**, 3206 (1981).
[52]E. F. Zalewski, R. A. Keller, and C. T. Apel, *Ibid.*, p. 1584.
[53]O. A. Novodvorskiĭ, "Mechanisms of ionization and formation of an optogalvanic signal in a flame accompanying interaction with resonance radiation," Author's Abstract of Candidate's Dissertation, Moscow State University, Moscow (1984).
[54]A. S. Gonchakov, N. B. Zorov, Yu. Ya. Kuzyakov, and O. I. Matveev, Anal. Lett. **12**, 1037 (179); Zh. Anal. Khim. **37**, 520 (1982).
[55]P. K. Schenk, J. C. Travis, and G. C. Turk, J. Phys. (Paris) **44**, C7-75 (1983); Progr. Anal. Atom. Spectr. **7**, 241 (1984).
[56]Th. Berthoud, N. Drin, J. Lipinsky, and P. Camus, J. Phys. (Paris) **44**, C4-67 (1983).
[57]T. Berglin and L. Casparsson, *Ibid.*, p. 329.
[58]K. C. Smyth and W. G. Mallard, J. Chem. Phys. **77**, 1779 (1982).
[59]O. A. Novodvorskiĭ, N. B. Zorov, Yu. Ya. Kuzyakov, and A. P. Palivoda in: Abstracts of Reports at the 19th All-Union Conference on Spectroscopy, Tomsk (1983), Vol. 5, p. 17.
[60]I. M. Beterov and N. N. Fateev, J. Phys. (Paris) **44**, C7-487 (1983).
[61]G. Hertz, Z. Phys. **18**, 307 (1923).
[62]K. H. Kingdon, Phys. Rev. **21**, 408 (1923).
[63]D. Popescu, I. Popescu, and J. Richter, Z. Phys. **226**, 160 (1969).
[64]B. M. Smirnov, Vozbuzhdennye atomy (Excited Atoms), Energoizdat, M.(1982).
[65]K. C. Harvey, Rev. Sci. Instr. **52**, 104 (1981).
[66]R. Beigang and A. Timmerman, J. Phys. (Paris) **44**, C7-137 (1983).
[67]K. Niemax and C. J. Lorenzen, Opt. Commun. **44**, 165 (1983).
[68]S. Moffat and A. L. S. Smith, *Ibid.*, **37**, 119 (1981).
[69]S. Moffat and A. L. S. Smith, J. Phys. D **17**, 59 (1984).
[70]R. E. Munchausen, R. D. May, and G. W. Hill, Opt. Commun. **48**, 317 (1984).
[71]N. K. Zaĭtsev and N. Ya. Shaparev, Zh. Tekh. Fiz. **55**, 210 (1985) [Sov. Phys. Tech. Phys. **30**, 122 (1985)].
[72]R. Nowicki and J. Pienkowski, J. Phys. D **15**, 1165 (1982).
[73]A. L. S. Smith and S. Moffat, *Ibid.* **17**, 71 (1984).
[74]E. Arimondo, M. G. DiVito, and M. Inguscio, J. Phys. (Paris) **44**, C7-267 (1983).
[75]E. M. Van Veldhuisen, The Hollow Cathode Glow Discharge Analyzed by Optogalvanic and Other Studies: Thesis, Eindhoven (1983).
[76]S. N. Atutov, I. M. Ermolaev, and A. M. Shalagin, Pis'ma Zh. Eksp. Teor. Fiz. **40**, 374 (1984) [JETP Lett. **40**, 1185 (1984)].
[77]F. Kh. Gel'mukhanov and A. M. Shalagin, Kvant. Elektron. **8**, 590 (1981) [Sov. J. Quantum Electron. **11**, 357 (1981)].
[78]A. I. Parkhomenko and V. E. Prokop'ev, Opt. Spektrosk. **53**, 1000 (1982) [Opt. Spectrosc. (USSR) **53**, 597 (1982)].
[79]V. S. Letokhov and V. P. Chebotaev, Printsipy nelineĭnoĭ lazernoĭ spektroskopii (Principles of Nonlinear Laser Spectroscopy), Nauka, M. (1975).
[80]J. E. M. Goldsmyth, A. I. Ferguson, J. E. Lawler, and A. L. Shawlow, Opt. Lett. **4**, 230 (1979).
[81]C. J. Lorenzen, K. H. Weber, and K. Niemax, Opt. Commun. **33**, 271 (1980).
[82]K. Niemax, Acta Phys. Pol. A **61**, 517 (1982).
[83]J. E. Lawler, A. I. Ferguson, J. E. M. Goldsmyth, D. J. Jackson, and A. L. Shawlow, Phys. Rev. Lett. **42**, 1046 (1979).
[84]T. W. Hansch, D. R. Lyons, A. L. Shawlow *et al.*, Opt. Commun. **38**, 47 (1981).
[85]C. Wieman and T. W. Hansch, Phys. Rev. Lett. **36**, 1170 (1976).
[86]R. E. Teets, F. V. Kowalski, W. T. Hill *et al.*, Proc. Soc. Photo-Opt. Instrum. Eng. **113**, 80 (1977).
[87]Ph. Dabkiewicz and T. W. Hansch, Opt. Commun. **38**, 351 (1981).
[88]L. Julien and M. Pinard, J. Phys. B **15**, 2881 (1982).
[89]M. Pinard and L. Julien, J. Phys. (Paris) **44**, C7-129 (1983).
[90]D. R. Lyons, A. L. Schawlow, and G. Y. Yan. Opt. Commun. **38**, 35 (1981).
[91]Ch. Belfrage, P. Grafstrom, S. Kroll, and S. Svanberg, J. Phys. (Paris) **44**, C7-169 (1983).
[92]G. W. Series, Comm. At. Mol. Phys. **10**, 199 (1981).
[93]L. R. Pendrill, M. Pettersson, and U. Osterberg, J. Phys. (Paris) **44**, C7-489 (1983).
[94]J. N. Dodd, J. Phys. B **16**, 2721 (1983).
[95]F. Strumia, J. Phys. (Paris) **44**, C7-117 (1983).
[96]P. Hannaford, D. S. Gough, and G. W. Series, *Ibid.*, C7-107.
[97]M. P. Chaika, Opt. Spektrosk. **39**, 1015 (1975), **40**, 628 (1976) [Opt. Spectrosc. (USSR) **39**, 582 (1975); **40**, 359 (1976)]. N. G. Preobrazhenskiĭ and A. E. Suvorov, "Hanle effect in a semitransparent gas," Preprint No. 2-78, Institute of Theoretical and Applied Mechanics of the Siberian Branch of the USSR Academy of Sciences, Novosibirsk (1978).
[98]G. C. Turk, J. C. Travis, J. R. DeVoe, and T. C. O'Haver, Analyt. Chem. **51**, 1890 (1979).
[99]J. E. M. Goldsmyth, Opt. Lett. **7**, 437 (1982).
[100]G. C. Turk, W. G. Mallard, P. K. Schenk, and K. C. Smyth, Analyt. Chem. **51**, 2408 (1979).
[101]P. Camus, M. Dieulin, A. E. Himdly, and M. Aymar, Phys. Scripta **27**, 125 (1983).
[102]C. R. Vidal, Opt. Lett. **5**, 158 (1980).
[103]K. Miyazaki, H. Scheingraber, and C. R. Vidal, Phys. Rev. A **28**, 2229 (1983).
[104]C. Hameau, J. Wascat, D. Dangoisse, and P. Glorieux, Opt. Commun. **49**, 423 (1984).
[105]S. A. Brunker and S. C. Haydon, J. de Phys. **44**, C7-55 (1983).
[106]J. E. M. Goldsmyth, *Ibid.*, C7-87.
[107]A. E. Bulyshev and N. G. Preobrazhenskiĭ in: All-Union Symposium on Computational Tomography, Computing Center and Institute of Theoretical and Applied Mechanics of the Siberian Branch of the USSR Academy of Sciences, Novosibirsk (1983), p. 16.
[108]V. V. Pikalov and N. G. Preobrazhenskiĭ, Usp. Fiz. Nauk **141**, 469 (1983) [Sov. Phys. Usp. **26**, 974 (1983)].
[109]V. V. Pikalov and N. G. Preobrazhenskiĭ, Izv. Akad. Nauk SSSR, Ser. Fiz. **48**, 1289 (1984) [Bull. Acad. Sci. USSR Phys. Ser. **48**(7), 40 (1984)].
[110]C. J. Lorenzen, K. Niemax, and L. R. Pendrill, Opt. Commun. **39**, 271 (1980).
[111]K. Niemax and L. R. Pendrill, J. Phys. B **13**, 461 (1980).
[112]L. R. Pendrill and K. Niemax, *Ibid.* **15**, 147 (1982).
[113]C. J. Lorenzen and K. Niemax, Phys. Scripta **27**, 300 (1983).
[114]C. J. Lorenzen and K. Niemax, J. Phys. B **15**, 139 (1982).
[115]K. Niemax, Appl. Phys. B **32**, 59 (1983).
[116]C. J. Lorenzen and K. Niemax, Z. Phys. K1. **A311**, 249 (1983).
[117]C. J. Lorenzen and K. Niemax, Opt. Commun. **43**, 26 (1982).
[118]R. A. Keller, R. Engleman, and E. F. Zalewski, J. Opt. Soc. Am. **69**, 738 (1979).
[119]P. Pianarosa, Y. Demers, and J. M. Gagne, J. Opt. Soc. Am. **B1**, 704 (1984).
[120]H. Rinneberg and J. Neukammer, J. Phys. (Paris) **44**, C7-177 (1983).
[121]F. Penent, C. Chardonnet, D. Delande, F. Biraben, and J. C. Gay, *Ibid.*,

C7-193.
[122]J. P. Lemoigne, J. P. Grandin, X. Husson, and H. Kucal, *Ibid.*, C7-209.
[123]C. B. Collins, *Ibid.*, C7-395.
[124]C. B. Collins, S. M. Curry, B. W. Johnson, M. Y. Mirza, M. A. Chellechmalzadeh, J. A. Anderson, D. Popescu, and I. Popescu, Phys. Rev. A **14**, 1662 (1976).
[125]M. Y. Mirza and W .W. Duley, Proc. R. Soc. London A **364**, 255 (1978).
[126]M. Y. Mirza and W. W. Duley, Opt. Commun. **28**, 179 (1979).
[127]M. A. Chellechmalzadeh and C. B. Collins, Phys. Rev. A **19**, 2270 (1979).
[128]C. B. Collins, F. W. Lee, H. Golbani, F. Davanloo, P. A. Vicharelli, D. Popescu, and I. Popescu, J. Chem. Phys. **85**, 1105 (1981).
[129]P. K. Schenk, W. G. Mallard, J. C. Travis, and K. C. Smyth, J. Chem. Phys. **69**, 5147 (1978).
[130]D. Feldman, Opt. Commun. **29**, 67 (179).
[131]T. Suzuki, *Ibid.* **38**, 364 (1981).
[132]C. T. Rettner, C. R. Webster, and R. N. Zare, J. Phys. Chem. **85**, 1105 (1981).
[133]I. M. Beterov and N. V. Fateev, Opt. Commun. **40**, 425 (1982).
[134]C. Demuynck and J. L. Destombes, IEEE J. Quantum Electron. **QE-17**, 575 (1981).
[135]I. M. Beterov and N. V. Fateev, Opt. Spektrosk. **54**, 978 (1983) [Opt. Spectrosc. (USSR) **54**, 580 (1983)].
[136]J. Pfaff, M. Begemann, and R. J. Saykally, Bull. Am. Phys. Soc. **27**, 11 (1982).
[137]Yu-Min Wang, Zhen-xing Gui, and Shun-yi Zhang, Chinese Phys. **2**, 799 (1982).
[138]M. C. Scolnick, IEEE J. Quantum Electron. **QE-6**, 139 (1970).
[139]A. L. S. Smith and S. Moffat, Opt. Commun. **30**, 213 (1979).
[140]M. J. Kavaya, R. T. Mensies, and U. P. Oppenheim, IEEE J. Quantum Electron. **QE-18**, 19 (1982).
[141]W. E. Bell and A. L. Bloom, J. Appl. Phys. **32**, 906 (1961).
[142]A. C. Tam, IEEE Trans. Plasma Sci. **10**, 252 (1982).
[143]O. I. Matveev, N. B. Zorog, and Yu. Ya. Kuzyakov, Talanta **27**, 907 (1980).
[144]D. Apostol and C. Blanary, Rev. Roum. Phys. **27**, 581 (1982).
[145]A. Sasaki, S. Usimaru, and T. Hayashi, Japan. J. Appl. Phys. **24**, 593 (1984).
[146]Laser Frequency Stabilizer, Laser Focus **19**, 147 (1983).
[147]G. D. Lobov, V. V. Shtykov, V. I. Bogatkin, and L. V. Drugov, Radiotekh. Elektron. **17**(6), 1247 (1972) [Radio Eng. Electron. (USSR) **17**, 968 (1972)].
[148]R. B. Green, R. A. Keller, G. G. Luther, P. K. Schenk, and J. C. Travis, IEEE J. Quantum Electron. **QE-13**, 63 (1977).
[149]V. S. Burakov, A. A. Gvozdev, P. Ya. Misakov, P. A. Naumenko, and S. N. Raĭkov in: Ref. 59, Vol. 1, p. 271.
[150]C. A. Hamer and J. P. Spoonhower, Appl. Spectr. **38**, 212 (1984).
[151]D. C. King, P. K. Schenk, K. C. Smyth, and J. C. Travis, Appl. Opt. **16**, 2617 (1977).
[152]R. A. Keller, R. E. Engleman, and B. A. Palmer, *Ibid.* **21**, 1468 (1982).
[153]J. R. Nestor, J. Phys. (Paris) **44**, C7-387 (1983).
[154]C. R. Webster, Appl. Opt. **21**, 2298 (1982).
[155]A. Ben-Amar, R. Shuker, and G. Erez, Appl. Phys. Lett. **38**, 763 (1981).
[156]S. Avriller and J. P. Sherman, Opt. Commun. **19**, 87 (1976).
[157]I. M. Beterov and N. V. Fateev in: Lazernye sistemy (Laser Systems), Institute of Theoretical Physics of the Siberian Branch of the USSR Academy of Sciences, Novosibirsk (1982), p. 121.
[158]I. M. Beterov, V. A. Kurochkin, and N. V. Fateev, Zh. Khim. Fiz. **1**, 957 (1982).
[159]J. C. White, R. R. Freeman, and P. F. Liao, Opt. Lett. **5**, 120 (1980).
[160]K. H. Weber and K. Niemax, Z. Phys. K1. **A307**, 13 (1982); **A309**, 19 (1982).
[161]K. Niemax, Appl. Phys. B **32**, 59 (1983).
[162]R. A. Zhitnikov in: Abstracts of Review Reports at the 6th All-Union Conference on Low-Temperature Plasma Physics, Leningrad, 1983, p. 83.
[163]F. O. Shimizu, K. Sasaki, and K. Ueda, Japan, J. Appl. Phys. **22**, 1144 (1983).
[164]R. Klein, P. McGinnis, and R. Leone, Chem. Phys. Lett. **100**, 475 (1983).
[165]H. A. Bachor, P. J. Manson, and R. J. Sandeman, Opt. Commun. **43**, 337 (1982).
[166]H. O. Behrens and G. H. Guthohrlein, J. Phys. (Paris) **44**, C7-149 (1983).
[167]D. K. Otorbaev, V. N. Ochkin, N. G. Preobrazhenskiĭ, S. Yu. Savinov, A. I. Sidel'nikov, and N. N. Sobolev, Zh. Eksp. Teor. Fiz. **81**, 1626 (1981) [Sov. Phys. JETP **54**, 865 (1981)].
[168]R. B. Green, R. A. Keller, P. K. Schenk, J. C. Travis, and G. C. Luther, J. Amer. Chem. Soc. **98**, 1517 (1976).
[169]P. K. Schenk and K. C. Smyth, J. Opt. Soc. Am. **68**, 626 (1978).
[170]C. A. van Dijk, P. J. Th. Seegers, G. Nienhuis, and C. Th. Alcemade, J. Quantit. Spectr. Rad. Transfer. **20**, 55 (1978).
[171]Yu. Ya. Kuzyakov, N. B. Zorov, V. I. Chaplygin, and O. A. Novodvorsky, J. Phys. (Paris) **44**, C7-335 (1983).
[172]G. C. Turk, J. C. Travis, and J. R. de Voe, *Ibid.*, C7-301.
[173]J. C. Travis, G. C. Turk, and R. B. Green, Analyt. Chem. **54**, 1006 (1982).
[174]Th. Berthoud, P. Camus, N. Drin, and J. L. Stehle, J. Phys. (Paris) **44**, C7-389 (1983).
[175]V. I. Chaplygin, "Laser atomic-ionization method for determining traces of potassium, rubidium, and cesium with atomization of the sample in a flame," Author's Abstract of Candidate's Dissertation, Moscow State University, M., 1984.
[176]M. Kushner, Appl. Opt. **22**, 1970 (1983).
[177]N. Ya. Shaparev, Zh. Tekh. Fiz. **49**, 2229 (1979) [Sov. Phys. Tech. Phys. **24**, 1230 (1979)].
[178]Sh. M. Kogan and T. M. Lifshits, Phys. Status Solidi A **29**, 11 (1977).
[179]R. B'yub, Fotoprovodimost' tverdykh tel (Photoconductivity of Solids), Fizmatgiz, M., 1962.
[180]N. S. Kopeika and J. Rosenbaum, IEEE Trans. **PS-4**, 51 (1976).
[181]N. S. Kopeika, *Ibid.* **PS-6**, 261 (1978).
[182]V. I. Balykin, G. I. Bekov, V. S. Letokhov, and V. I. Mishin, Usp. Fiz. Nauk **132**, 293 (1980) [Sov. Phys. Usp. **23**, 651 (1980)].
[183]V. S. Antonov, V. S. Letokhov, and A. N. Shibanov, Usp. Fiz. Nauk **142**, 177 (1984) [Sov. Phys. Usp. **27**, 81 (1984)].
[184]V. S. Letokhov, Priroda, No. 2, 15 (1985).

Translated by M. E. Alferieff